# MAE 4273: EXPERIMENTAL FLUID DYNAMICS

***Lab Report***

***Fall 2019***

**Particle Image Velocimetry (PIV) Study of Flat Plate Boundary Layer**

School of Mechanical and Aerospace Engineering

Oklahoma State University

November 27, 2019

**ABSTRACT** [250 words maximum]

Boundary layer theory suggests a relatively thin layer of fluid flow relative to the flow length over an object exists and varies with Reynolds number. The boundary layer thickness depends with fluid properties, flow velocity, and flow length over a surface, and exact and approximate solutions exist for calculating the boundary layer properties. This laboratory will characterize boundary layer effects and determine the boundary layer thickness for a range of Reynolds numbers from $6x10^4$ to $6x10^5$ for flow inside a 30cm x 30cm water tunnel. Particle Image Velocimetry (PIV) was used to non-intrusively capture flow photos and analyze them using the PIVlab toolbox in MATLAB. An acrylic flat plate was used as the bottom flow surface, and a second trial was conducted with a 1.27cm diameter acrylic half rod at the flat plate leading edge to induce boundary layer trip. Downstream locations spanning 8.89cm to 16cm from the flat plate leading edge were tested across freestream velocities from 3.9cm/s to 34.2cm/s. The experiment showed variation in the horizontal velocity profiles, and the freestream velocity and boundary layer thickness definitions likely over-estimated the actual boundary layer thickness, thereby providing a poor approximation of laminar or turbulent flow estimates. The trip condition resulted in boundary layers with more velocity fluctuation and greater thickness than the no trip condition. The boundary layer effects were quantified, and the influence of Reynolds number was observed and validated against the Reynolds number equation definition.

## 1. INTRODUCTION AND OBJECTIVES

1. Utilize PIV to characterize the flow quality of the OSU ATRC 059 30cm water tunnel for variation of horizontal velocity with respect to flow height from 0 to 10cm
2. Determine the effect of boundary layer growth and turbulence along a flat plate up and downstream between 8.89cm and 16cm from the flat plate leading edge
3. Quantify boundary layer thickness for a flat plate (no boundary layer trip) and 1.27cm-diameter half bar at the flat plate leading edge (intentional boundary layer trip)

## 2. EXPERIMENTAL ARRANGEMENTS

### *Materials:*

For this laboratory, both an acrylic flat plate and half round bar were used for altering flow behavior. The clear acrylic flat plate sat on the bottom of the water tunnel test section and was 0.25 inches (0.64cm) thick and 12 inches (30cm) along each edge. A schematic of this is shown in Figure 1. This flat plate was smoothed out with black Gorilla Tape to provide a clean ramp up from the test section entrance. In the second part of the laboratory, the clear half cylinder bar sat at the front of the flat plate and test section with flat side down. It measured 0.5 inches (1.27cm) in diameter and 12 inches (30cm) in length, spanning the width of the test section and is depicted in Figure 2. The purpose of the half cylinder was to trip the flow, and this is described in greater detail in the following paragraphs. Additionally, the coordinate system was defined to be at the start of the flat plate/cylinder origin as described by Figure 3. An overhead view is shown in Figure 4. The installation of this flat plate in the tunnel can be seen in Figure 5.

Dispersed in the flow were glass seeding particles: hollow spheres, 9-13 micrometers in diameter [1] and manufactured by LaVision (LaVision, Inc., Ypsilanti, MI, U.S.A) for use in water (P/N 110P8), Figure 6. These seeding particles are neutrally buoyant, flowing with the water throughout the tunnel for PIV purposes, yet not so large or numerous to disturb or alter the water flow over the plate and half cylinder in the tunnel. These particles function similarly to tracking markers in the entertainment industry that allow cameras to follow movement but are not so large that they alter an actor's movement or hide their features.

### *Facilities and Equipment:*

The water tunnel used in this study was the Oklahoma State University 30cm Flow Visualization Water Tunnel (Engineering Laboratory Design Inc., Lake City, MN, USA) located in ATRC 059. It features one enclosed impeller, stainless steel pump, belt driven by a 7.5 horsepower ODP (open drip proof) AC motor with a variable frequency controller for regulating the shaft RPM of each pump from 0.01m/s to 0.5m/s [2]. A second pump is also available for increasing the maximum flow speed to 1.0 m/s but was not necessary for this experiment. The test section is 30cm wide, 30cm high, 100cm long test section, clear all around and open at the top for insertion of test articles, such as the half bar used for tripping the boundary layer.

Multiple instruments were used in this lab including a camera, laser, sheet optics and mirror, and high-speed controller. The Phantom Miro LAB110 camera (Ametek. Wayne, NJ, USA) obtained photos of the flow at a high frame rate to capture the particle movement. It contained a 1280x800 resolution, 12-bit pixel depth, 1600 FPS frame rate, sensor size of 25.6mm x 16.0mm, and temporal resolution minimum exposure of 2 microseconds [3]. The lens was a Nikon AF Nikkor 50mm 1:1.4D set to 0.45ft as seen in Figure 7.

The laser was a 1W DPSSL Class 4 Laser. Its purpose was to provide the necessary illumination for identifying particles in the water tunnel flow. Operating in the 532nm wavelength, the beam quality was less than 2 $M^2$, a beam diameter of 1-2mm, and beam divergence of <1.5mrad [4]. The unit is manufactured by LaVision. The laser (Figure 8) is operated by the DPSSL Driver (Figure 9) and on its own only produces a circular beam which is not useful in PIV. However, when coupled with the associated optics and mirror, an illuminated sheet is produced that cleanly identifies a cross section of the water tunnel flow. These are discussed in the following paragraphs.

To convert the laser's circular beam into a sheet, a laser scanner (manufactured by LaVision) assembly contains a 20-facet high-reflectivity mirror that rapidly rotates, creating an imperceptible strobe effect that appears to the unaided eye as a single sheet spanning a cross section of the water tunnel. A schematic of this assembly is depicted in Figure 10. This is useful for the high-speed camera that is focused on the thin illuminated cross section in the middle of the tunnel and can be seen in Figure 11.

Because of the high frame rate (discussed in the following section), and minimal camera on-board storage, each burst of photo captures is transferred through the LaVision Highspeed controller (Figure 12) to be stored on the connected computer. The controller also dictates when frames are to be captured, when, and at which speed. The controller is operated via the DaVis software program, version 8.3.0. Owned by LaVision, it is licensed to Oklahoma State University throughout this experiment and features the hardware support, Highspeed camera support, and 2D PIV packages. The dongle number is 12912, order number KA14116, and version ID 8870 [5].

***Experimental protocols:***

This laboratory setup began by taking the overall dimensions of the water tunnel test section and measuring the position of the camera relative to the tunnel walls as shown in Figure 4. The camera lens was also measured to ensure its perpendicularity to the tunnel. This was accomplished by measuring each horizontal end of the camera lens to the water tunnel walls and rotating the camera mount to achieve the same distance from all parts of the lens. For this experiment, the camera had previously been positioned correctly, so perpendicularity was confirmed with these measurements. A level was also used to confirm the camera's horizontal position with respect to the water tunnel flow. The flat plate had also been previously secured to the floor of the tunnel test section with Gorilla Tape, providing the smooth ramp up to the 0.25 inch thick plate. Next, the laser was turned on and the resulting illuminated sheet was tweaked to confirm that it was not only centered in the tunnel's width, but also normal to the tunnel walls in the same manner as the camera lens. For the half cylinder trip condition, the half bar was secured to the tunnel at the start of the flat plate location as shown in Figure 2.

The seeding particles had been combined with the water in previous labs, but to ensure even distribution, the tunnel was turned on and allowed to flow for several minutes to remix the particles. Following even particle distribution, the camera was turned on in junction with the laser to focus the lens. To accomplish this, a black sheet was draped on the opposite side of the tunnel, so the camera did not pick up any additional objects or lights in the background. The camera was focused on the seeding particles illuminated by the laser and checking for any 3D distortion of the observed particle sheet. Following approval by the TA, the PIV target lowered into the water for calibrating the camera field of view as shown in Figure 13. Upon completion, the target was removed, and data acquisition could proceed.

The students began by executing the test matrix shown in Table 1. The first water tunnel pump speed of 5 Hz was selected, thereby beginning the tunnel flow speed. The flow was allowed to reach steady state before sending the PC command to the HighSpeed Controller to obtain an image burst off 500 photos at that moment. The organization of this data is described in Figure 14. This process was repeated several times, adjusting the frame rate as necessary to obtain a movement of 4 pixels between frames for a given particle. As the tunnel flow speed increased, the camera frame rate increased as well to

keep up with the more rapidly moving particles. The actual frame rate and corresponding time steps used are listed in Table 2. This process of increasing the tunnel's flow speed, allowing it to reach steady state, and obtaining a sample of images with a 4-pixel displacement between frames was repeated for 5, 10, 20, 30, and 40 Hz tunnel motor frequency.

Finally, this process was repeated but with the cylinder half bar in place to observe the significance of tripping flow and its effect on the boundary later. The water tunnel flow and laser were turned off while the TA secured the cylinder half bar to the front edge of the flat plate with Gorilla Tape. Once placed and checked for perpendicularity to the flow with a ruler, the tunnel flow and laser could be turned on again. The same test matrix was executed as previously, using the same motor frequency and frame rates for consistency. This final run concluded data acquisition of the experiment.

***Postprocessing:***

Following image data acquisition, image processing was conducted to extract position and velocity information from the particle imaging obtained in the laboratory. The raw data consisted of 500 black and white photographs taken with the Phantom Miro LAB110 camera for each configuration of no-trip/trip and tunnel speed. An example photo is shown in Figure 15 for 5Hz tunnel speed without the half-bar trip. Utilizing the PIVlab v2.31 (Thielicke, W. and Stamhuis, E.J., 2014) toolbox for MATLAB (MathWorks, Natick, MA, USA), the images were loaded, pre-processed, analyzed, calibrated, post-processed, and exported for analysis by MATLAB or another program such as Microsoft Excel (Microsoft Corporation, Redmond, WA, USA).

In PIVlab, batches of photos for each tunnel frequency were imported from the landing page using the "1-2, 2-3, 3-4, …" sequencing style. Exclusions and masks were then added to prevent analysis of the stationary flat plate within the camera field of view (FOV). For all frames throughout this laboratory, a mask was applied to the bottom of each frame which contained the flat plate lower boundary for the water flow. Additionally, a reduced region of interest (ROI) was applied because a characteristic of this laboratory setup was an issue with the flow imaging. As seen in Figure 16, unsteady flow behavior is observed in each frame for the left-hand side of the captured FOV. While less drastic for the overall frame average (Figure 17), the flow quality nonetheless presented a concern. Reasoning for this is likely due to an experimental setup and lighting issue with the laser and/or camera. The camera may have been angled slightly, hence un-focusing the lens from the thin laser-illuminated sheet. While the flow itself was likely nominal, the means to measure the flow with PIV was compromised. This observation was addressed with Dr. Arvind Santhanakrishnan at Oklahoma State University, and a reduced ROI was approved for analysis of all frames of data. The original ROI was reduced from 942x556 pixels to 500x560 pixels to span the right-hand size of each frame only. This reduced ROI is shown in Figure 18.

For image pre-processing, contrast-limited adaptive histogram equalization (CLAHE) window size was enabled to 15px, high pass kernel size enabled to 12px, and auto-contrast stretch enabled between 0.192 and 1. PIV settings utilized the FFT window deformation algorithm with a first pass interrogation window size of 64px with a 50% step of 32. A second pass was enabled with a 32px area and 50% step of 16. The sub-pixel-estimator was the Gauss 2x3-point with normal correlation quality. With these pre-analysis settings applied, all frames were analyzed for each data set.

With imaging analysis complete, calibration was applied using the image shown in Figure 19. Each dot indicated a distance of 5mm, and the appropriate time step was applied for the corresponding configuration as shown in Table 2. This applied pixel measurements to the actual FOV which measured 7.68in x 4.72in (195mm x 120mm) for the photos which were 947x552 pixels, to result in 1 pixel equaling 0.18mm. After applying calibration, the mean of all frames was calculated and due to the lack of outlier vectors observed by inspection, no vector validation post-processing was applied. The mean of all frames was saved as a tab-delimited ASCII text file, and the cumulative PIVlab session was saved for each configuration should the PIVlab session need to be restored and/or modified.

***Calculated quantities:***

The following equations are utilized in this laboratory throughout data analysis and plots generation. As this laboratory focuses on boundary layer characterization, the boundary layer thickness $\delta$ is defined in Equation 1 as the *y* height perpendicular to the flow when the boundary layer velocity, *u*, is 99% of the freestream velocity, $U_\infty$.

$$\delta = y, \text{when } u = 0.99U_\infty \tag{1}$$

Reynolds number ($Re_x$) is a measure of the ratio of inertial to viscous forces and is defined in Equation 2. It will be used to describe the freestream flow in some plots as the *x* location may vary up or downstream. Reynolds number is therefore a better metric for interpreting figures because of its non-dimensionality. The length *x* is the downstream distance of interest and kinematic viscosity ν is defined as 9.757e-7$m^2$/s for water at 21°C [6].

$$Re_x = \frac{U_\infty x}{\nu} \tag{2}$$

In some plots, nondimensionalizing the velocity and position location (*x* or *y*) is helpful to determine how a local boundary layer velocity *u* relates to the freestream velocity $U_\infty$. This results in a percentage of boundary layer velocity to freestream velocity, and as $u/U_\infty$ approaches 1, the boundary layer velocity is nearly the same as the freestream, hence the boundary layer is considered no longer present. Its relationship to $y/\delta$ is calculated by Equation 3 where *n* is a best fit power law exponent that varies to fit experimental data. According to smooth turbulent boundary layer theory, *n* may be approximated as 1/7 or 0.14 for experimental values. This laboratory will compare PIV-obtained data to the 1/7 exponent approximation.

$$\frac{u}{U_\infty} = \left(\frac{y}{\delta}\right)^n \tag{3}$$

The Blasius solution approximates $\delta/x$ as a function of Reynolds number to the -1/2 power in Equation 4. It assumes two-dimensional, steady, incompressible fluid flow with constant velocity over a flat plate, as is the case for this laboratory. It also assumes a laminar boundary layer.

$$\frac{\delta}{x} = \frac{4.9}{\sqrt{Re_x}} \tag{4}$$

$\delta/x$ may also be approximated by Equation 5 for a turbulent boundary layer that forms by steady, incompressible and constant viscosity flow over a smooth plate with a sharp leading edge and zero pressure gradient. The data in this laboratory will be compared to the solutions given in both Equations 4 and 5.

$$\frac{\delta}{x} = 0.16Re^{-\frac{1}{7}} \tag{5}$$

To calculate the boundary layer displacement $\delta^*$, the following integral equation is used to integrate along the boundary layer thickness to the *y* location of freestream speed.

$$\delta^* = \int_0^\infty \left(1 - \frac{u}{U_\infty}\right) dy \tag{6}$$

Momentum thickness $\theta$ is calculated with Equation 7, and also completed by integrating from zero to the *y* location of freestream speed.

$$\theta = \int_0^\infty \frac{u}{U_\infty}\left(1 - \frac{u}{U_\infty}\right) dy \tag{7}$$

Shape factor is defined by Equation 8. The value of H for laminar flow is 2.59, but ranges from 1.3-1.4 for turbulent flow.

$$H = \frac{\delta^*}{\theta} \tag{8}$$

The application of these equations to data analysis is described in the following section.

## 3. RESULTS AND DISCUSSION

### *3.1. Summary:*

For data analysis, the flow quality was first assessed for each trial run by determining horizontal velocity as a function of flow height. This established horizontal velocity profiles to understand variances throughout the flow height, and how those profiles differed for increasing freestream velocity. Freestream velocities were used to determine the boundary layer thickness for the most downstream location of the ROI for each test configuration. Non-dimensionalized horizontal velocities were also plotted as a function of flow height where the flow variance observation was further validated. Finally, the results were compared to laminar and turbulent approximations and shown to not align well with those figures.

### *3.2. Effects of flow height on horizontal velocity:*

Following imaging analysis in PIVlab, the ASCII text files generated contained position and velocity data for all points from the calculated mean frame. Firstly, to validate the freestream speeds, the maximum recorded u velocity was compared to the water tunnel frequency calibration sheet [7]. These data are shown in Table 3 and match the calibration data well (percent differences are nearly all under 10%), hence it may be assumed the PIVlab calibration was correct and analysis may proceed.

Columns of *x*, *y*, *u*, and *v* data were imported into Excel, and 3 scatter plots generated for each the non-trip and trip conditions. The 3 plots for each condition spanned 3 different *x* locations: upstream, midstream, and downstream of the ROI. The varying *x* locations was to study the *x*-direction effects of these horizontal velocity profiles. Within each plot, all 5 freestream speeds were graphed to compare how increasing freestream velocity affects the velocity profiles as well.

The freestream velocity for each configuration was defined as the maximum *u* velocity value from each data set. This approach was chosen rather than selecting the *u* velocity value corresponding to the highest *y* distance because of the taper-off in velocity at the top of the flow field as shown in Figures 20-25 (and explained in the following paragraphs).

For the upstream location of *x*=0.08894m (from the leading edge of the FOV, not the ROI), Figure 20 indicates that with increasing freestream velocity, the horizontal velocity profile varies more in approaching the freestream. This horizontal velocity variation is indicative of the observed boundary layer. Additionally, there is a flow velocity taper off towards the top of the flow field that is more profound at higher freestream speeds. This may be an artifact of the illumination, that at higher flow speeds, the seeding particles aren't captured as well as at lower flow speeds. This lighting issue was discussed in the previous section when reducing the ROI in PIVlab due to the poor flow behavior

observed in the left-hand side of the FOV. Figure 21 examines the midstream location of $x$=0.1263m and further variance is prevalent at the higher freestream velocities, especially for 0.303m/s (pump frequency of 40Hz). The two lowest freestream velocities also begin to waver more in the apparent freestream. The flow quality appears the most chaotic and turbulent downstream at $x$=0.161m in Figure 22. There is increasing variance in horizontal velocity across all freestream speeds. For these 3 plots of the flat plate (no trip), it is observed that higher freestream speeds and increasing distance downstream correspond to more turbulence and variance in horizontal velocity pertaining to the boundary layer.

The same plots described above were also generated for the tripped condition. Figure 23 studies the same $x$ location of 0.08894m and a larger boundary layer is observed to extend up past 0.2m in the $y$-direction, whereas it only reached 0.1m or 0.15m for the no trip condition. In Figures 24 and 25 for the midstream and downstream locations, the maximum velocity for each freestream seems to be reduced the further downstream the flow goes. This is likely due to increased turbulence and vorticity and the flow velocity having increased vertical velocity, $v$, components, thereby reducing the $x$ component of velocity, $u$.

From these 6 plots for the no trip and trip conditions, the boundary layer effects seem greater for the tripped conditions. A larger horizontal velocity gradient exists that gets "dragged" along before it can reach the freestream velocity out of the boundary layer. At the higher flow speeds, turbulence seems to mix the flow more and causing it to appear less steady. There is less of a clear established laminar flow. The Reynolds numbers of these flows are discussed in the following sections and may relate to explaining the transition from laminar at low flow speeds to turbulence at higher tunnel speeds.

### *3.3. Effects of non-dimensionalized height on non-dimensionalized horizontal velocity:*

To study the similarity of the localized horizontal velocity throughout the boundary layer to the freestream velocity, a non-dimensionalized approach was utilized. This approach examines local position and velocity as a percentage of the maximum height and freestream velocity, respectively.

The freestream velocity determination used the same method described in the above section as the maximum $u$ velocity for each of the 10 data sets. From Equation 1, 99% of the freestream speed was calculated, and by interpolating the y location for 99%$U_\infty$, a boundary layer thickness was determined. This was completed for all 3 $x$ locations, but only the furthest downstream $x$ location was used for additional analysis and plotting. One issue with the $U_\infty$ definition is that there wasn't always a corresponding 99%$U_\infty$ large enough to satisfy the interpolation criteria. In this case, the largest $u$ value was selected at that $x$ location, and the corresponding $y$ distance was established as the boundary layer thickness. A complication of this approach is that the largest $u$ at the downstream $x$ location was often high up in the flow and resulted in a large boundary layer thickness. This method was applied to all 10 test conditions.

With the boundary layer thickness defined for each configuration, $u/U_\infty$ was calculated, as was $y/\delta$ with $U_\infty$ and $\delta$ held constant, and only varying the $u$ and $y$ values for each freestream profile. When plotted together, Figure 26 resulted and the fraction of $u/U_\infty$ was plotted as a result of varying $y/\delta$ throughout the flow height.

The variance that is observed is primarily the result of increased turbulence in the flow for higher Reynolds numbers. The faster flow facilitated mixing and reached more transition and even turbulent conditions. For each Reynolds number tested, a power law curve was applied, and the resulting equation added to the graph. Table 4 displays these best fit equations and studies the percent difference of the exponent $n$ to that of $n$=0.14 for smooth turbulent boundary layer. According to Table 4, the smallest Reynolds numbers ($Re<10^4$) were best approximated by this turbulent boundary layer. As Reynolds number increases and the flow should become more turbulent, the best fit power law equations approximate the flow more poorly. This may be best explained by the velocity profile variance throughout the flow height; the $u/U_\infty$ values fluctuate between 0.65 and nearly 1 over a small span and thereby lead to poor curve fitting, and hence poor comparison to the exponent $n$=0.14.

This same plot is also generated for the tripped condition in Figure 27. Similar trends in $u/U_\infty$ fluctuations exist, but the $u/U_\infty$ values vary even more, from 0.4 to nearly 1. The trip appears to facilitate additional flow mixing and turbulence which complicates the curve fitting as well.

These 2 plots comprised the non-dimensionalization of the flow height vs horizontal flow velocity.

### *3.4. Boundary layer comparison to laminar and turbulent flow:*

Additional non-dimensional quantities were examined by studying boundary layer thickness over $x$ position ($\delta/x$) vs Reynolds number. For each tested freestream Reynolds number, the local Reynolds number was calculated for each $x$ position step for the whole data set. These ranges of localized Reynolds numbers were plotted in Figure 28 for the no trip condition. All freestream Reynolds numbers follow a similar downward sloping trend, but when plotted against the laminar and turbulent boundary layer definitions from Equations 4 and 5, the $\delta/x$ quantity differs significantly. This is due to the large calculated boundary layer defined by the $U_\infty$ method described previously. The laminar and turbulent definitions were plotted to span the same Reynolds numbers as exhibited in the range of lowest to highest freestream Reynolds numbers.

The tripped condition is plotted in Figure 29 and features similar trends with a large difference from the laminar and turbulent approximations, also due to the large defined boundary layer.

### *3.5. Displacement thickness, momentum thickness, and shape factor:*

Flow quantities such as the displacement thickness, momentum thickness, and shape factor were also derived from the flow data and are tabulated in Table 5. Displacement thickness was calculated with Equation 6 using simple rectangular-stepped integration steps and summing the calculated areas to determine the thickness in meters. The integration was likewise completed using Equation 7 to determine the momentum thickness in meters. Lastly, the shape factor was computed and for values spanning 0.15 to 0.26, several freestream velocities fall into the turbulent flow criteria for $H$=1.3-1.4. These values were calculated for both the no trip and trip conditions.

### *3.6. Limitations:*

The limitations associated with this laboratory stem largely from the reduced ROI discussed in the Postprocessing section of Experimental Arrangements. The reduced ROI was unable to examine the leading edge of the flat plate and half bar trip. Boundary layer effects may have been more accurately analyzed in that region because further downstream where the analysis presented here began, more turbulent and disorderly flow likely existed.

The determination of $U_\infty$ as the maximum $u$ value for each data set was likely a source for error also affecting the boundary layer calculation. Because of the variance in horizontal flow as is best illustrated in Figure 26, the boundary layer thickness was defined as being much larger than it likely actually was. This cascaded into the poor alignment with the laminar and turbulent flow trends seen in Figures 28 and 29. It could be that tighter vector validation in the PIVlab postprocessing may have alleviated this issue.

For improving this study, a more rigorous definition of $U_\infty$ is necessary so that the actual, smaller boundary layer thickness is computed and then further utilized in plotting. The boundary layer thickness found in this study for each freestream velocity was likely too large for being 0.16m downstream of the flat plate and half bar for trip.

## 4. CONCLUSIONS

- Boundary layer analysis downstream yields more unsteadiness and variation of horizontal velocity profiles
- Tripping a boundary layer by means of a half bar results in a larger horizontal velocity profile variation. It requires increased flow height to achieve the freestream velocity.
- Flows may reach horizontal velocities near the freestream velocity, but then slow down for changing vertical flow height. This is likely due to turbulence and flow mixing as a result of the downstream data analysis.
- Variations in the horizontal flow velocity complicate validation to laminar or turbulent approximations of boundary layer thickness.

## REFERENCES

[1] "Seeding Particles: Glass Hollow Spheres." LaVision Inc. Ypsilanti, MI. https://www.lavision.de/en/applications/fluid-mechanics/piv-system-components/seeding-particles/.
[2] "Oklahoma State University: 30cm Flow Visualization Water Tunnel." Engineering Laboratory Design Inc. Lake City, MN. April 22, 2014.
[3] "Phantom Miro LAB-, LC- and R-Series Cameras Data Sheet." Ametek. Wayne, NJ.
[4] "DPSS Laser." LaVision Inc. Ypsilanti, MI.
[5] "About DaVis 8.3.0." LaVision GmbH. Goettingen, GER.
[6] "Water – Dynamic and Kinematic Viscosity." Engineering Toolbox. https://www.engineeringtoolbox.com/water-dynamic-kinematic-viscosity-d_596.html.
[7] "Water Tunnel Verification Test Data." Oklahoma State University. January 15, 2015.

**TABLES**

| Configuration | Pump Frequency $f_{pump,1}$ [Hz] | Pump Frequency $f_{pump,2}$ [Hz] | $U_\infty$ [m/s] | $Re_x$ |
|---|---|---|---|---|
| Without trip | 5 | 0 | 0.038 | 6242 |
| | 10 | 0 | 0.079 | 13514 |
| | 20 | 0 | 0.154 | 25401 |
| | 30 | 0 | 0.228 | 37526 |
| | 40 | 0 | 0.303 | 49658 |
| With trip | 5 | 0 | 0.039 | 6359 |
| | 10 | 0 | 0.079 | 12970 |
| | 20 | 0 | 0.158 | 26869 |
| | 30 | 0 | 0.230 | 37623 |
| | 40 | 0 | 0.342 | 56303 |

**Table 1:** Test Matrix of water tunnel pump frequency and the calculated freestream velocity and Reynolds number for each flow, with and without the half bar boundary layer trip.

| $U_\infty$ [m/s] | $Re_x$ (x $10^4$) | Recording rate [frames/s] | Time Step [ms] | PIV Algorithm | Interrogation Area [pixels] | | Overlap [%] |
|---|---|---|---|---|---|---|---|
| | | | | | Pass 1 | Pass 2 | |
| 0.038 | 0.63 | 80 | 12.5 | FFT Window Deformation | 64 | 32 | 50 |
| 0.079 | 1.32 | 150 | 6.67 | | | | |
| 0.156 | 2.61 | 300 | 3.33 | | | | |
| 0.229 | 3.76 | 400 | 2.5 | | | | |
| 0.323 | 5.30 | 500 | 2 | | | | |

**Table 2:** PIVlab analysis conditions. PIV settings for analysis algorithm and interrogation window area were maintained constant for all analyses. Overall FOV was 195mm x 120mm but the ROI was reduced to 500x560 pixels as discussed in the above lab report body for the 500 frames for each test condition.

| Pump *f* [Hz] | PIVlab max *u* ($U_\infty$) [m/s] | Pump 1 Spec [m/s] | Pump 2 Spec [m/s] | % diff to Pump 1 | % diff to Pump 2 |
|---|---|---|---|---|---|
| 5 | 0.038 | 0.0435 | 0.0412 | 13.5 | 8.1 |
| 10 | 0.079 | 0.0857 | 0.0808 | 8.1 | 2.3 |
| 20 | 0.156 | 0.1686 | 0.1585 | 7.8 | 1.6 |
| 30 | 0.229 | 0.2501 | 0.2346 | 8.8 | 2.4 |
| 40 | 0.323 | 0.3304 | 0.3095 | 2.3 | 4.3 |

**Table 3:** Comparison of the PIVlab-calculated freestream speed to the water tunnel specifications. Only 1 pump was running, but it was not determined which pump it was. The data appears to align best with pump 2 running only, as pump frequencies 10-40Hz all have percent differences under 5%.

| Reynolds Number | Trip Condition | Excel Power Curve | $(u/U_\infty) = (y/\delta)^n$ | $n$ %diff | $R^2$ |
|---|---|---|---|---|---|
| 6242 | No Trip | *y=1.5017x^6.185* | *x=0.94y^0.162* | 15% | 0.3694 |
| 13514 | | *y=1.32x^4.5033* | *x=0.94y^0.222* | 45% | 0.2996 |
| 25401 | | *y=1.283x^3.321* | *x=0.93y^0.3* | 73% | 0.0528 |
| 37526 | | *y=1.3045x^3.7674* | *x=0.932y^0.26* | 60% | 0.1555 |
| 49658 | | *y=1.285x^2.896* | *x=0.92y^0.34* | 83% | 0.161 |
| 6359 | Trip | *y=1.4343x^4.69* | *x=0.926y^0.21* | 40% | 0.7785 |
| 12970 | | *y=1.969x^5.3* | *x=0.88y^0.19* | 30% | 0.8173 |
| 26869 | | *y=1.55x^4.64* | *x=0.91y^22* | 44% | 0.8621 |
| 37623 | | *y=1.25x^3.73* | *x=0.94y^0.27* | 63% | 0.7551 |
| 56303 | | *y=1.693x^2.699* | *x=0.82y^0.37* | 90% | 0.7822 |

**Table 4:** Scaled Boundary Layer Power Law Curve Comparisons. The smooth boundary layer condition for n=0.17 is best approximated by the no trip, low Reynolds number condition. The $R^2$ fit is closest for the no trip condition as well.

| Motor *f* (Hz) | U∞ (m/s) | x (m) | $Re_x$ | $\delta_{99,smooth}$ (m) | $\delta^*_{99,smooth}$(m) | $\theta_{smooth}$ (m) | $\theta_{smooth}/\delta_{99,smooth}$ | $H_{smooth}$ |
|---|---|---|---|---|---|---|---|---|
| 5 | 0.038 | 0.161 | 6242 | 0.055 | 0.010 | 0.008 | 0.151 | 1.214 |
| 10 | 0.079 | 0.161 | 13514 | 0.057 | 0.012 | 0.009 | 0.161 | 1.256 |
| 20 | 0.154 | 0.161 | 25401 | 0.052 | 0.012 | 0.010 | 0.197 | 1.170 |
| 30 | 0.228 | 0.161 | 37526 | 0.055 | 0.012 | 0.010 | 0.185 | 1.198 |
| 40 | 0.303 | 0.161 | 49658 | 0.055 | 0.015 | 0.012 | 0.217 | 1.256 |
| | | | | | | | | |
| Motor *f* (Hz) | U∞ (m/s) | x (m) | $Re_x$ | $\delta_{99,tripped}$ (m) | $\delta^*_{tripped}$ (m) | $\theta_{tripped}$ (m) | $\theta_{tripped}/\delta_{99,tripped}$ | $H_{tripped}$ |
| 5 | 0.039 | 0.161 | 6359 | 0.067 | 0.015 | 0.011 | 0.170 | 1.309 |
| 10 | 0.079 | 0.161 | 12970 | 0.055 | 0.015 | 0.012 | 0.213 | 1.293 |
| 20 | 0.158 | 0.161 | 26869 | 0.057 | 0.013 | 0.010 | 0.178 | 1.317 |
| 30 | 0.230 | 0.161 | 37623 | 0.066 | 0.015 | 0.011 | 0.168 | 1.369 |
| 40 | 0.342 | 0.161 | 56303 | 0.067 | 0.027 | 0.017 | 0.262 | 1.574 |

**Table 5:** Displacement and momentum thickness, shape factor for the no trip and trip conditions. In the Reynolds number calculations, kinematic viscosity of water at 21°C was used = 9.757e-7 $m^2/s$.

## FIGURES

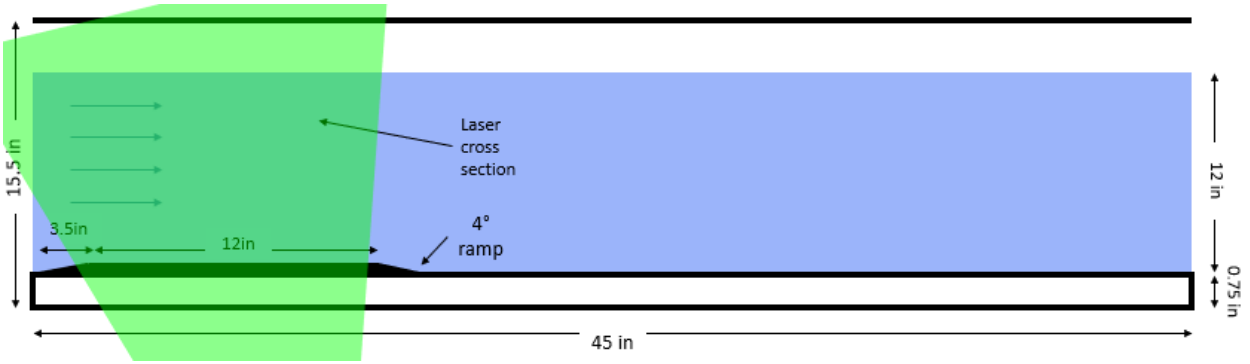


**Figure 1:** Water tunnel schematic with dimensions of flat plate locations

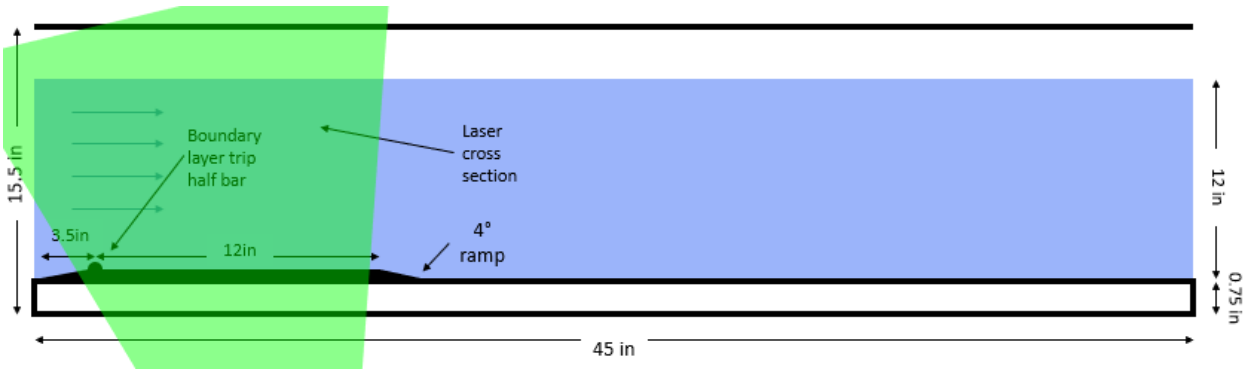


**Figure 2:** Water tunnel schematic with dimensions of cylinder half bar location.

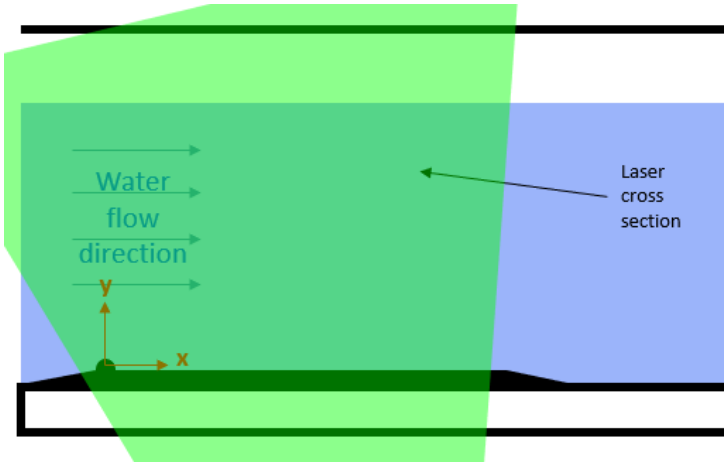


**Figure 3:** Test section side view indicating coordinate system location relative to cylinder half bar.

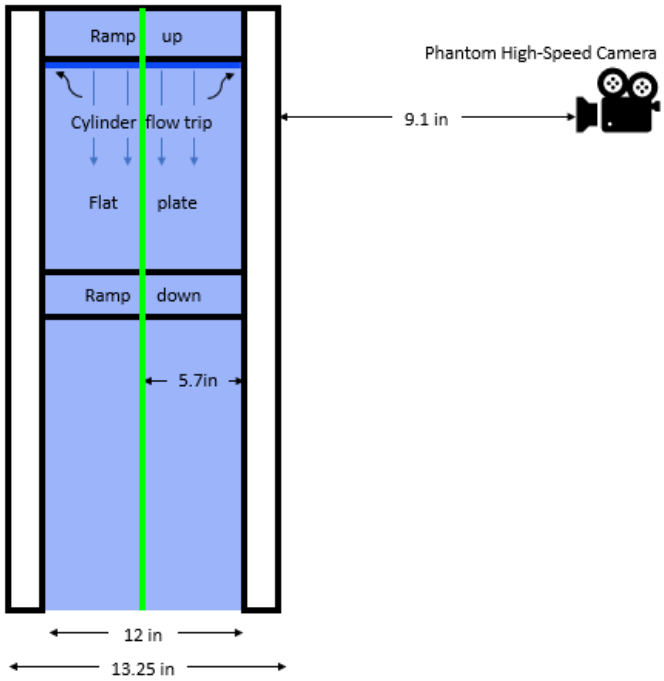


**Figure 4:** Overhead view of water tunnel west section with flat plate and cylinder half bar configurations shown.

**Figure 5:** Photo of the flat plate secured to the floor of the water tunnel test section entrance.


**Figure 6:** Photo of the LaVision glass seeding particles used.


**Figure 7:** Photo of the Ametek High Speed Camera with Nikon lens affixed.

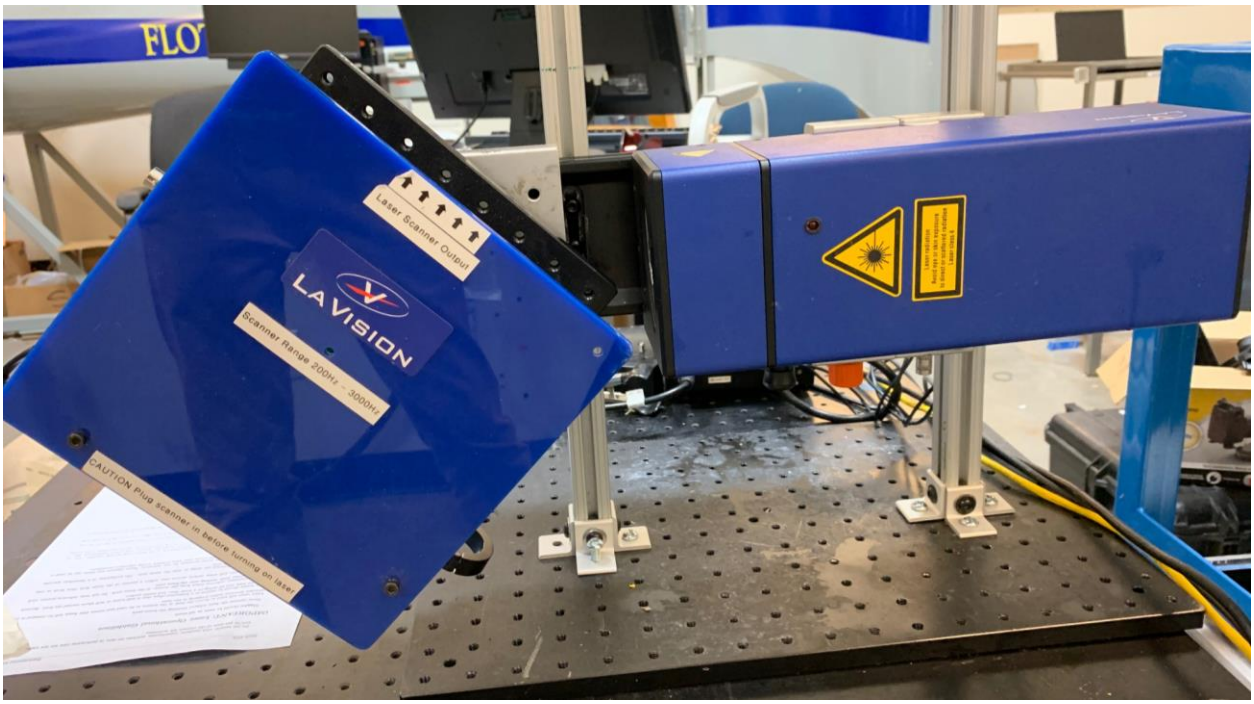


**Figure 8:** Photo of the LaVision 1W Class 4 Laser.


**Figure 9:** Photo of the LaVision DPSSL Laser Driver.

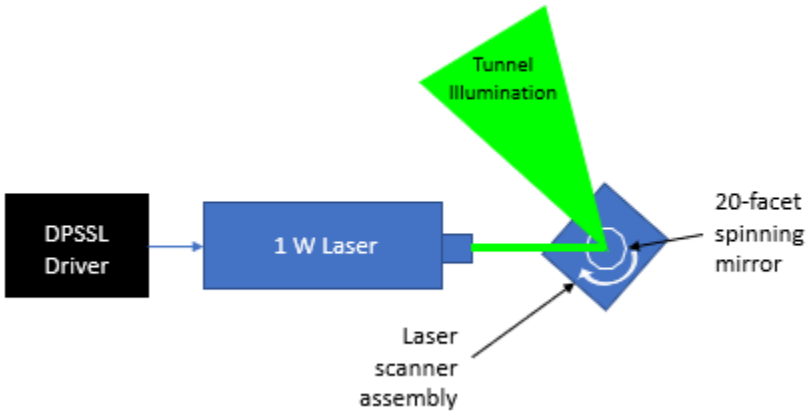


**Figure 10:** Schematic of laser system from power supply (DPSSL Driver) to laser and scattering.

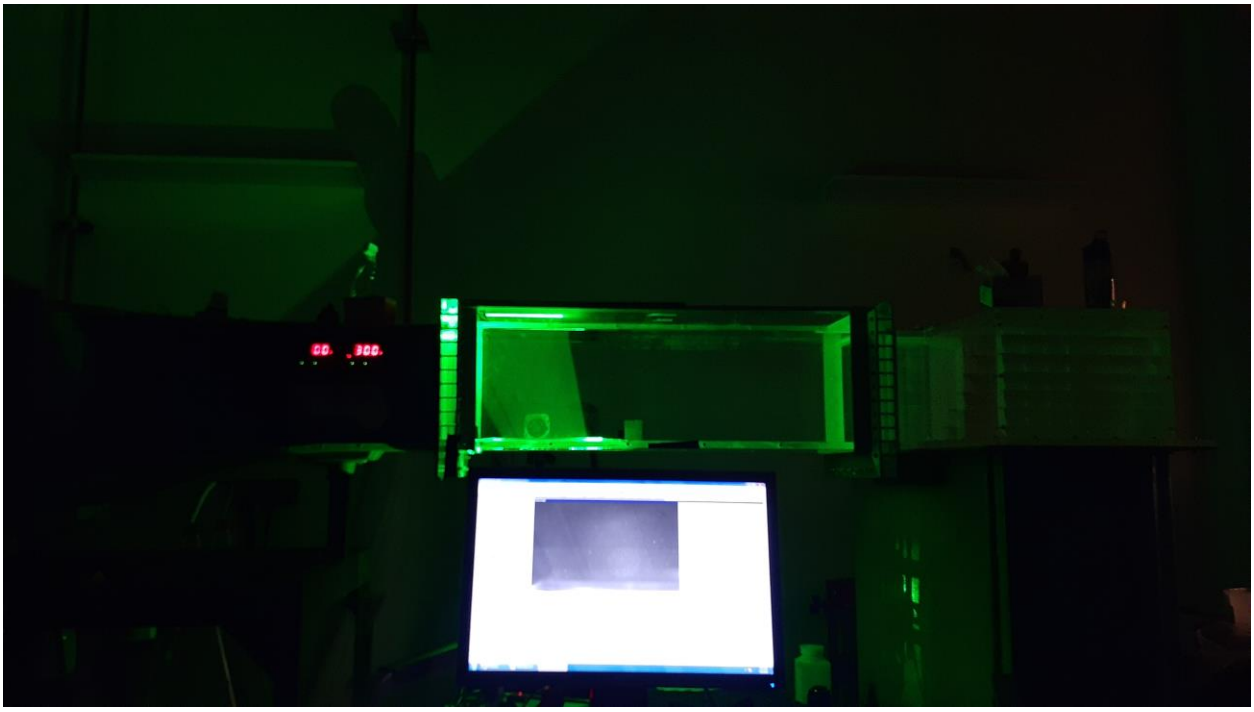

**Figure 11:** Photo of PIV setup with laser in action; illuminated sheet is visible through water tunnel.


**Figure 12:** Photo of the LaVision HighSpeed Controller.

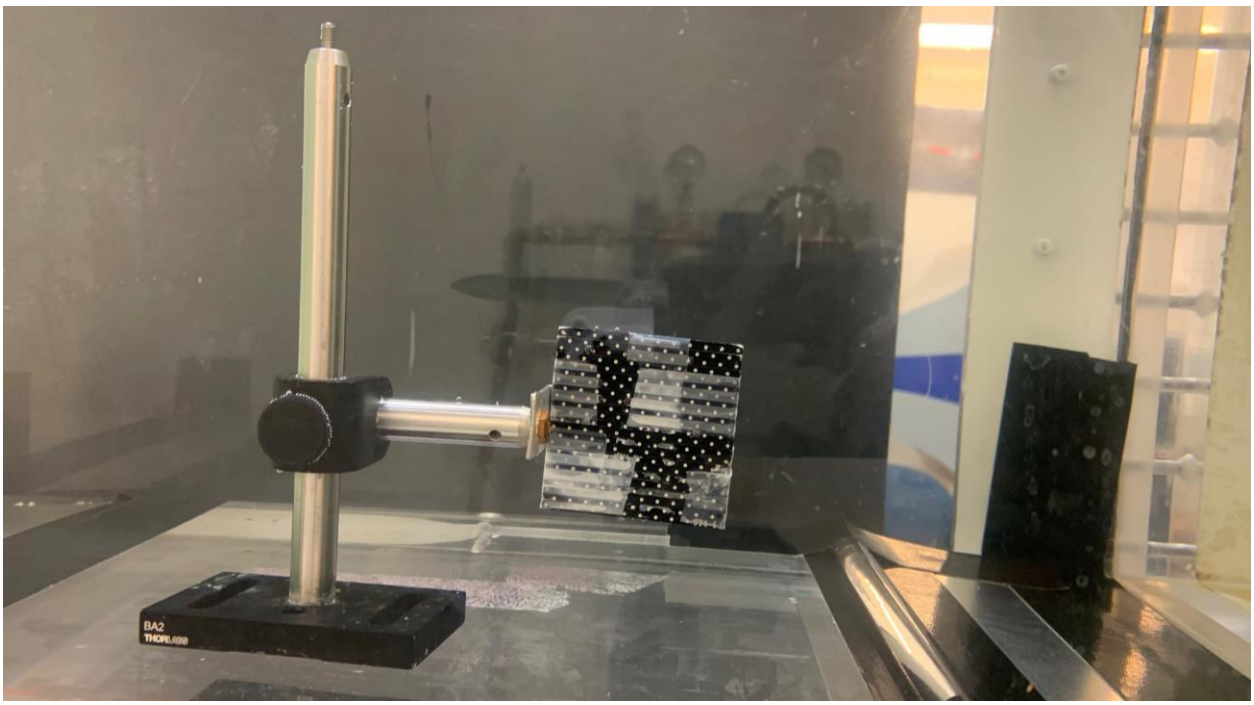

**Figure 13:** Photo of the PIV target used for calibration purposes.

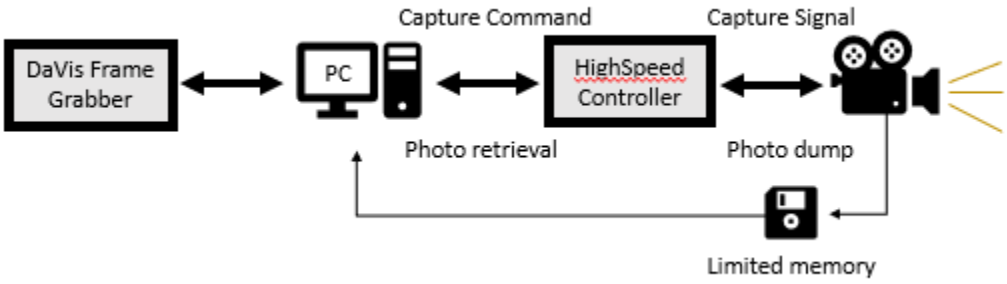


**Figure 14:** Schematic of high-speed camera data transfer and interaction with memory and PC for acquisition and control of image capturing.

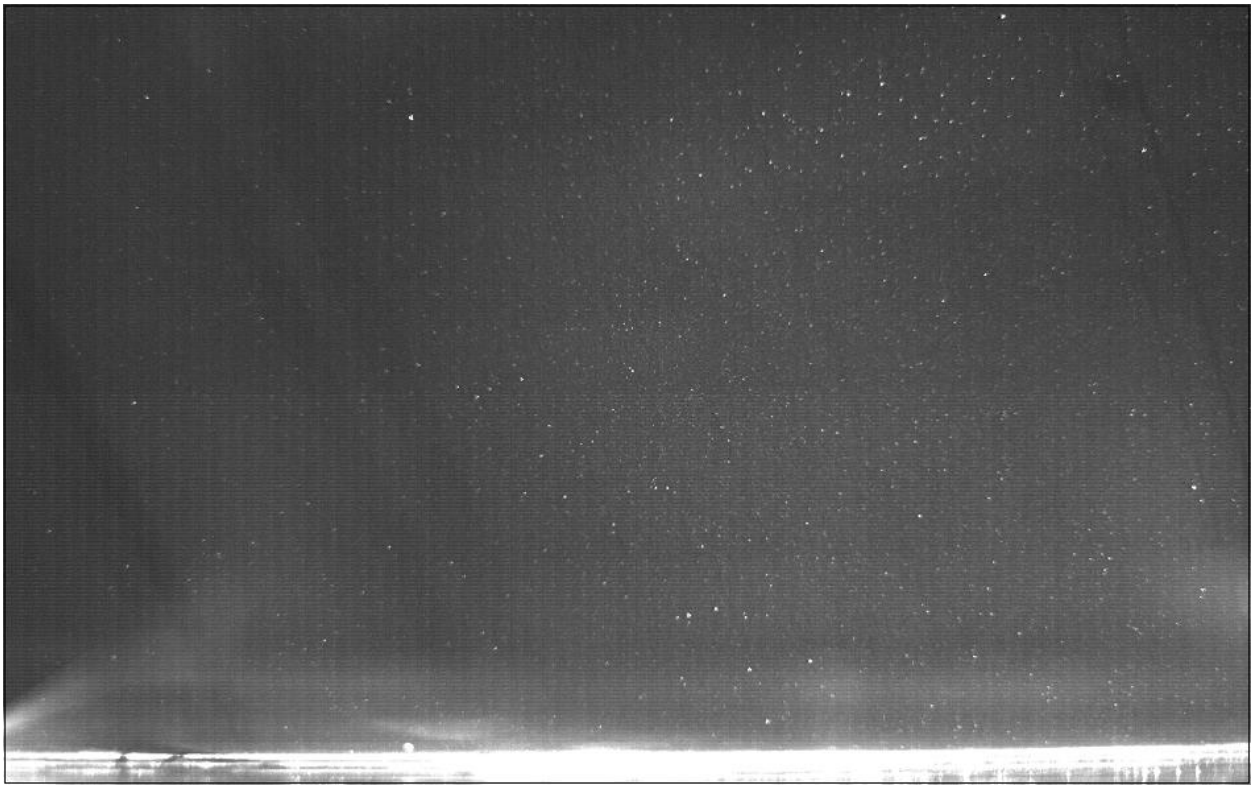

**Figure 15:** Sample image obtained from the camera that is then imported into PIVlab for data analysis. Flat plate is shown along the bottom edge, and white seeding particles are illumined in the flow.

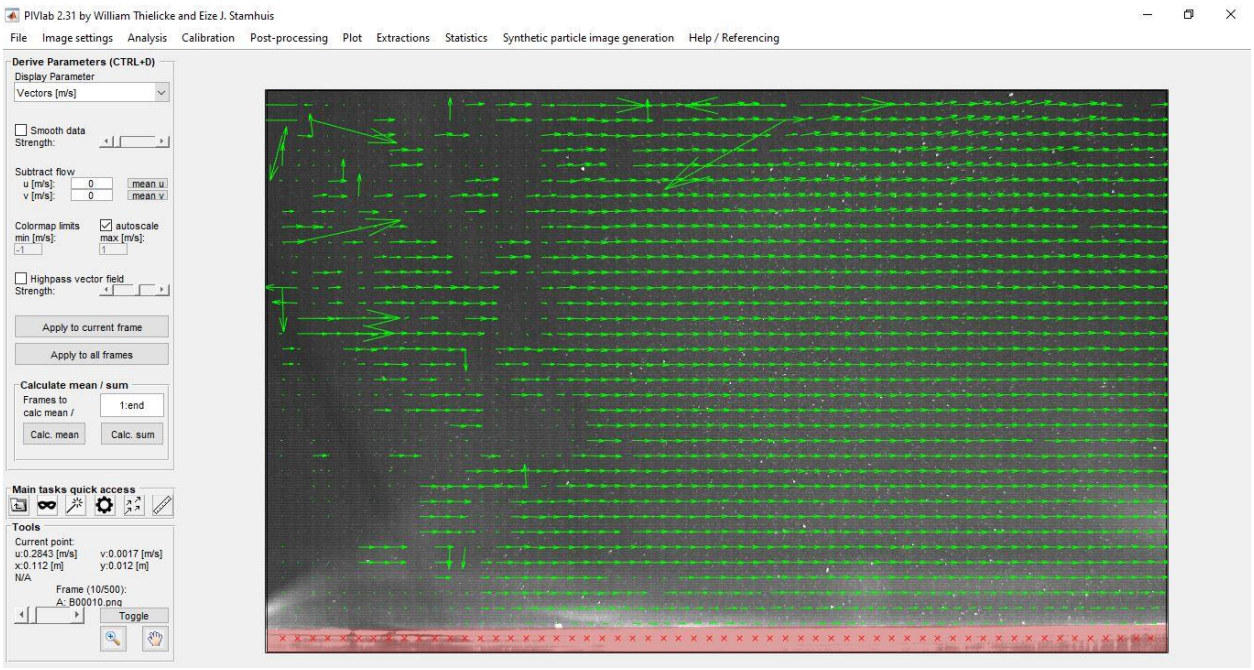


**Figure 16:** Frame analyzed in PIVlab at 5Hz without trip. Unusual flow behavior is visible on the left-hand side and would make for poor flow analysis and boundary layer characterization.

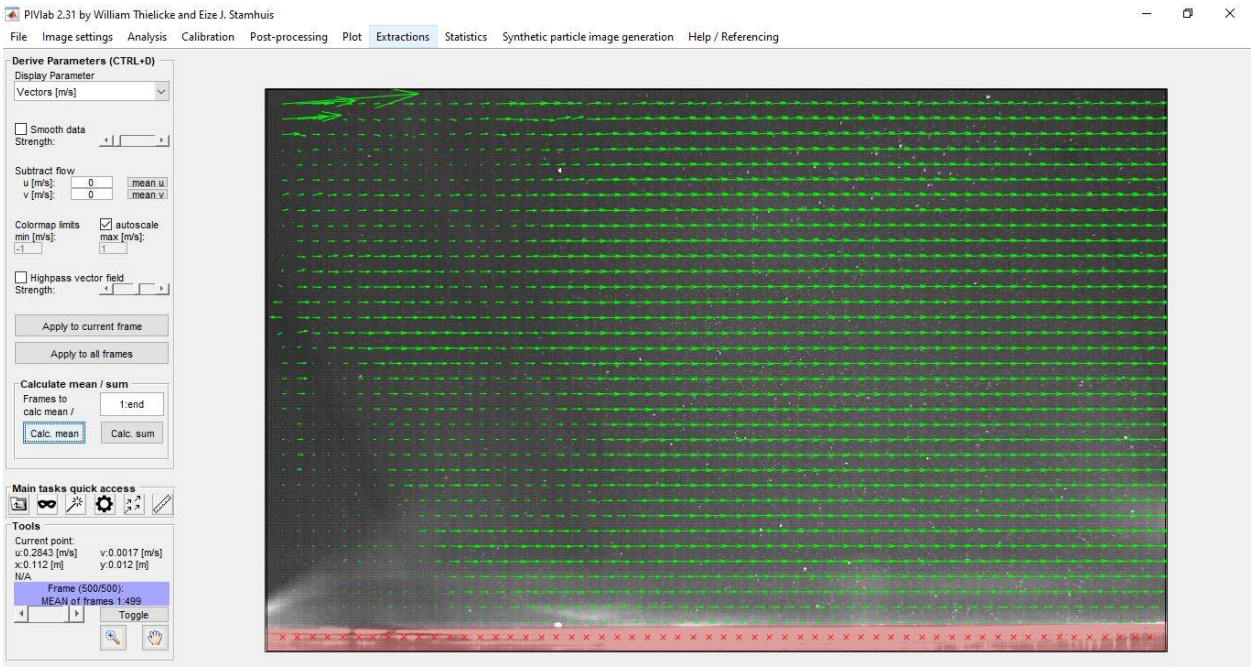


**Figure 17:** The mean of 500 frames at 5Hz, no trip is better than the individual frame analysis, but poor quality flow is still appears on the left.

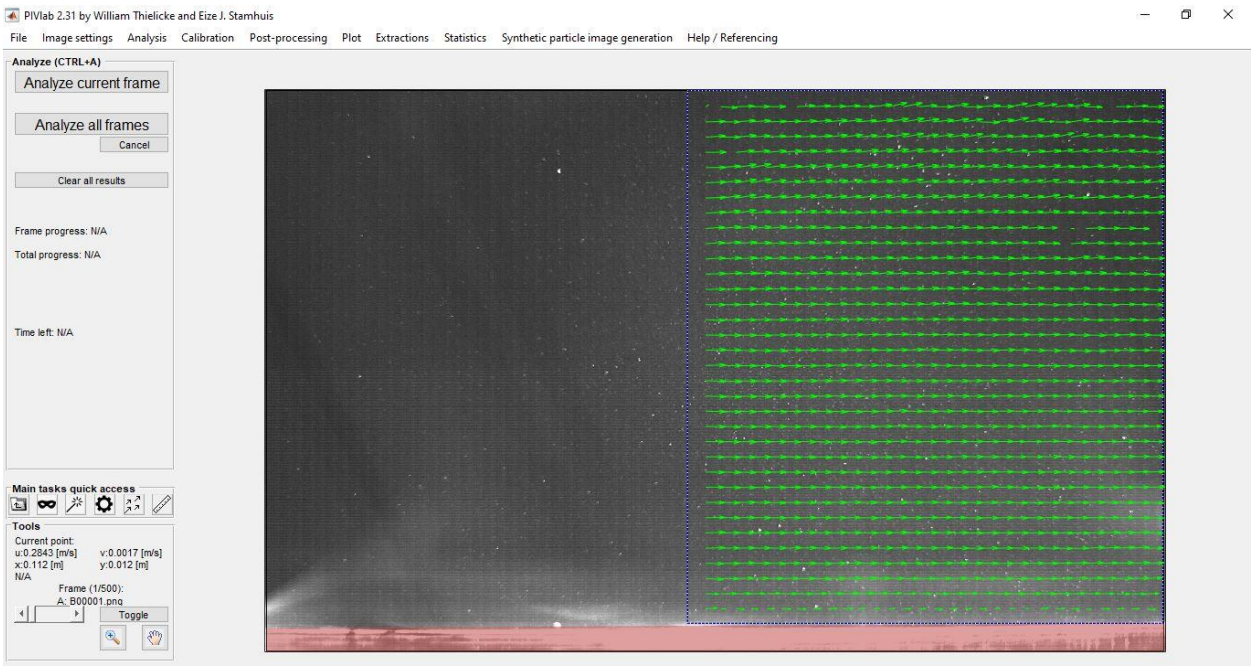


**Figure 18:** The reduced ROI utilizes the right-hand side of the FOV only. The mask is still applied along the bottom to remove any potential for flat plate velocity analysis.

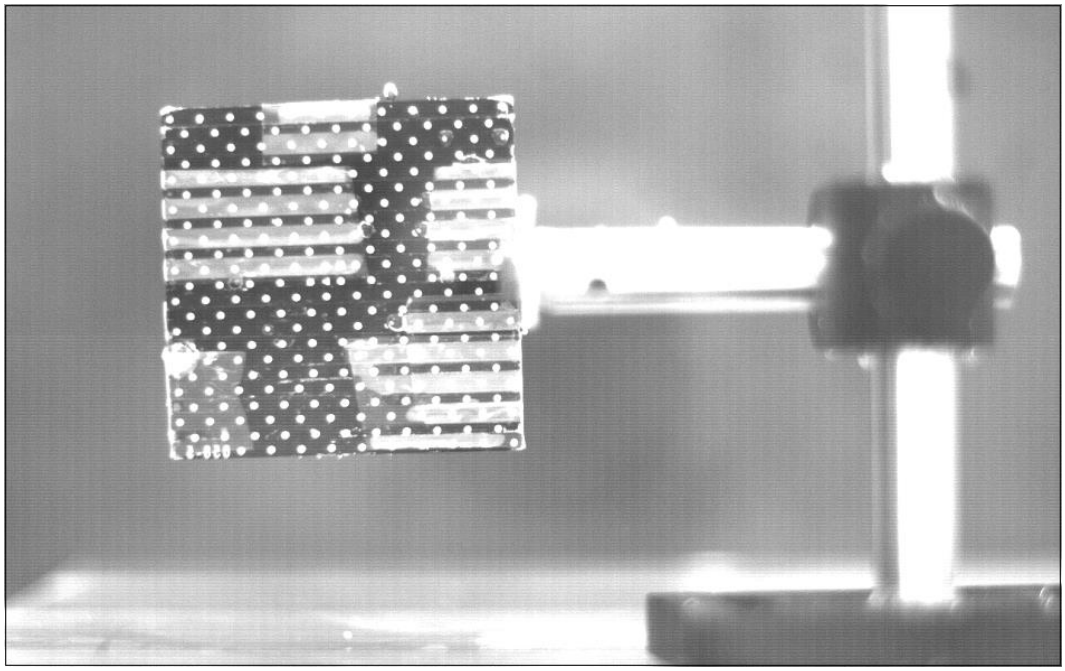

**Figure 19:** Calibration image used to apply calibration in PIVlab after analysis. Each dot measures 5mm between the next dot.

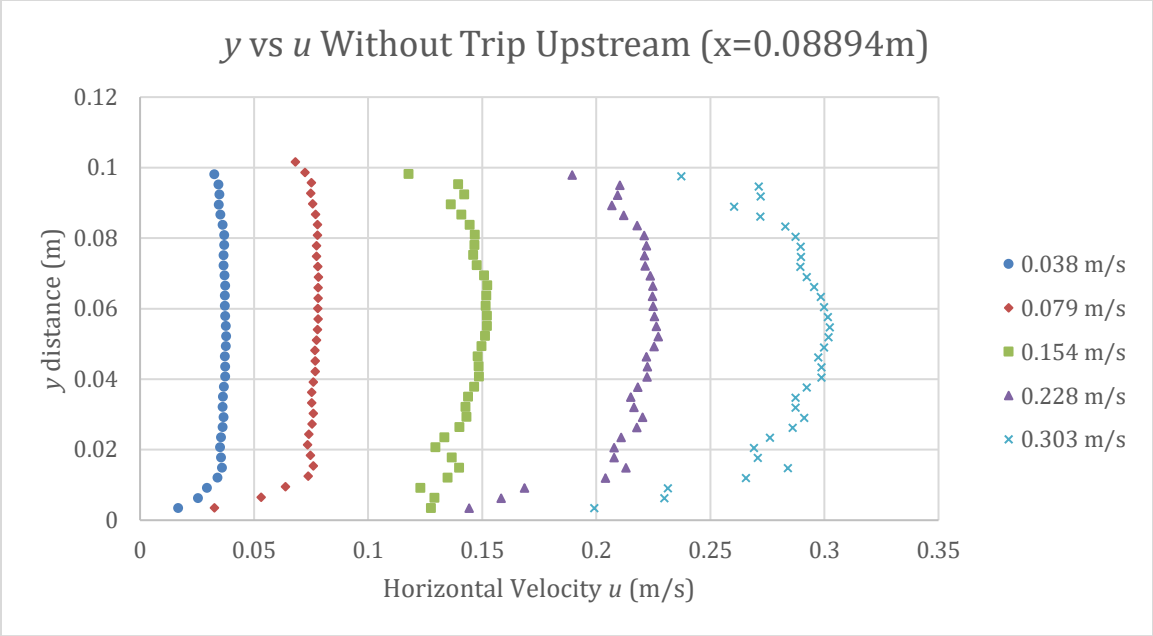


**Figure 20:** Horizontal velocity profile for the upstream location x=0.08894. Greater boundary layer effects seem prevalent for increased freestream speed.

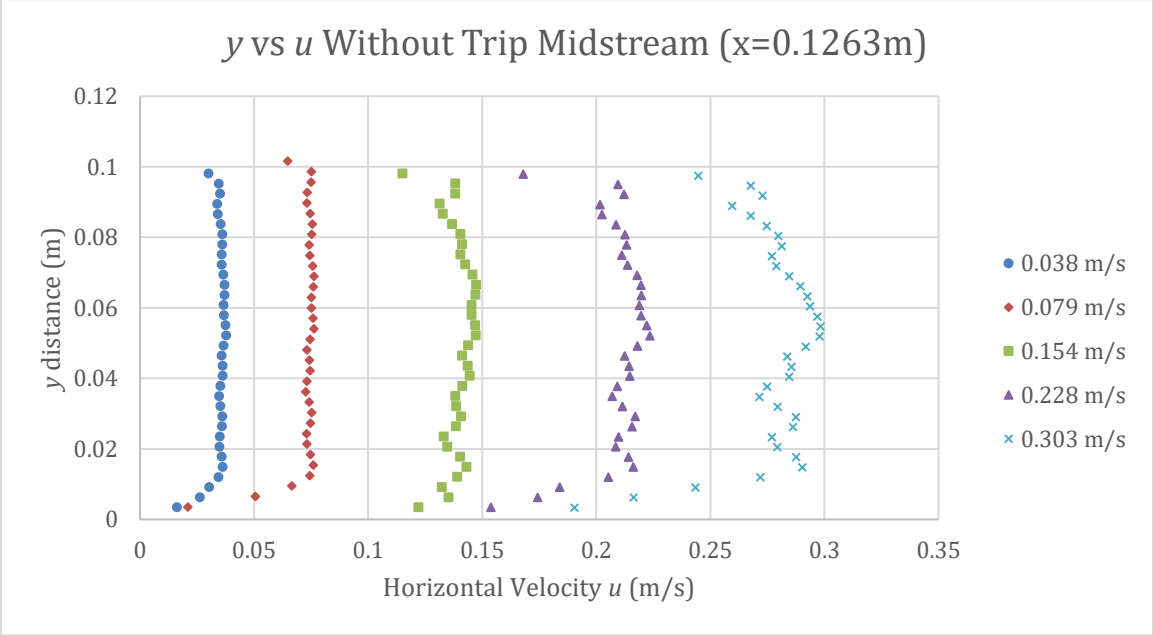


**Figure 21:** Horizontal velocity profile for the midstream location x=0.1263m. The horizontal velocity varies more with height y at higher freestream speed, especially for 0.303m/s.

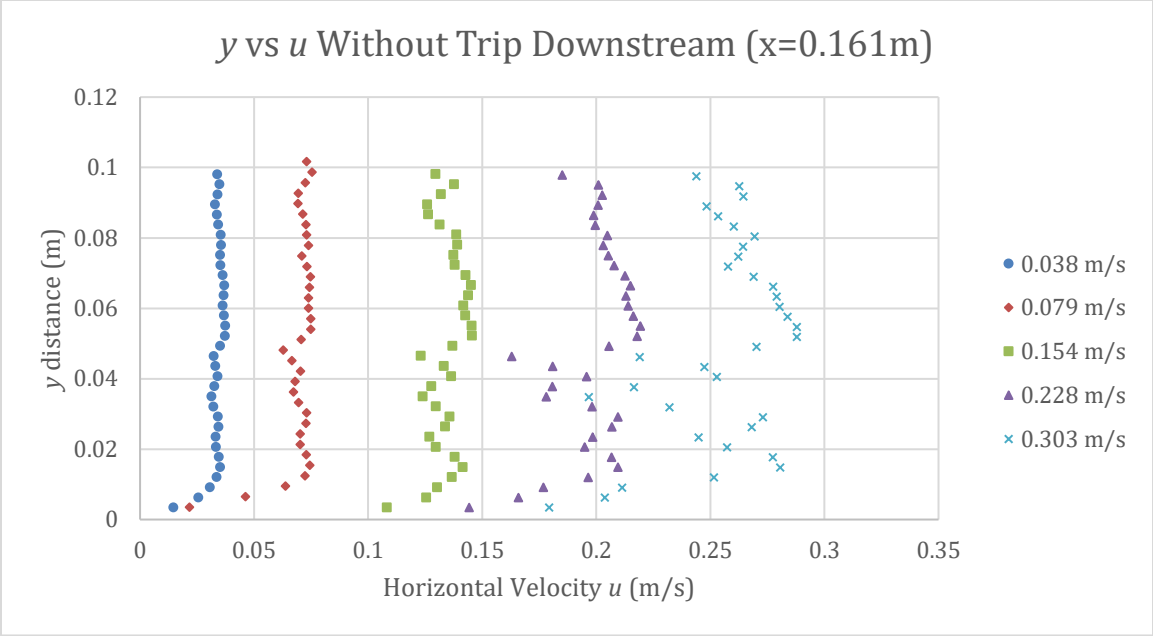


**Figure 22:** Horizontal velocity profile for the downstream location at x=0.161m. The velocity profiles at the highest 2 freestream speeds 0.228 and 0.303m/s exhibit great fluctuations midway up the ROI.

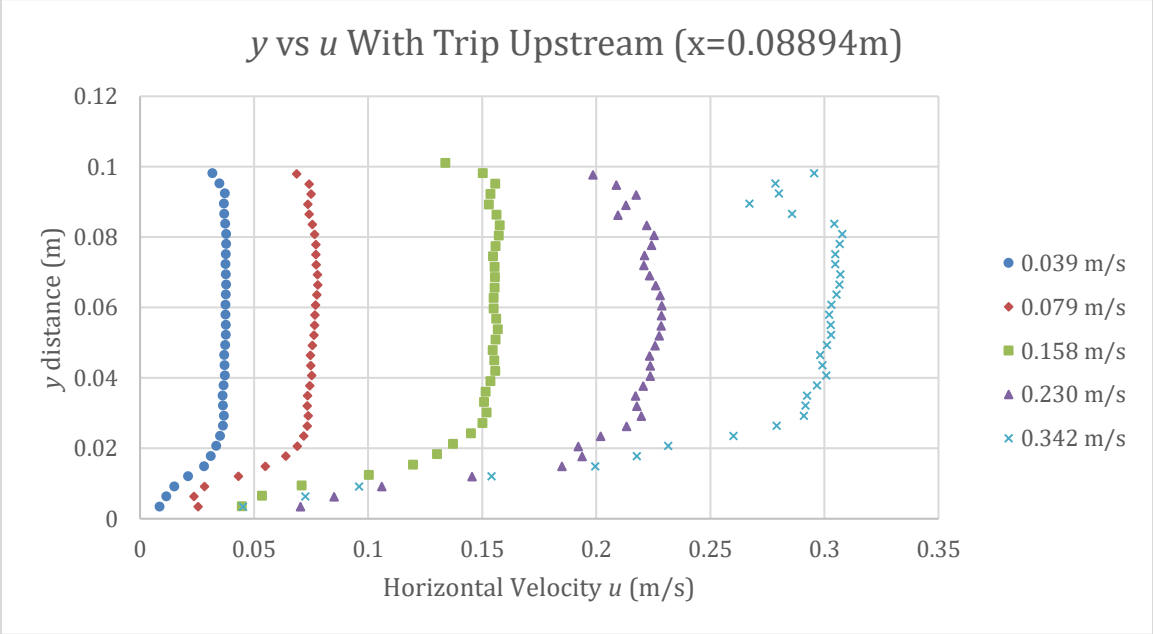


**Figure 23:** Horizontal velocity profile for the upstream location at x=0.08894m with half bar trip. Boundary layer thickness greater due to the effect of trip, especially at high freestream speed 0.342m/s.

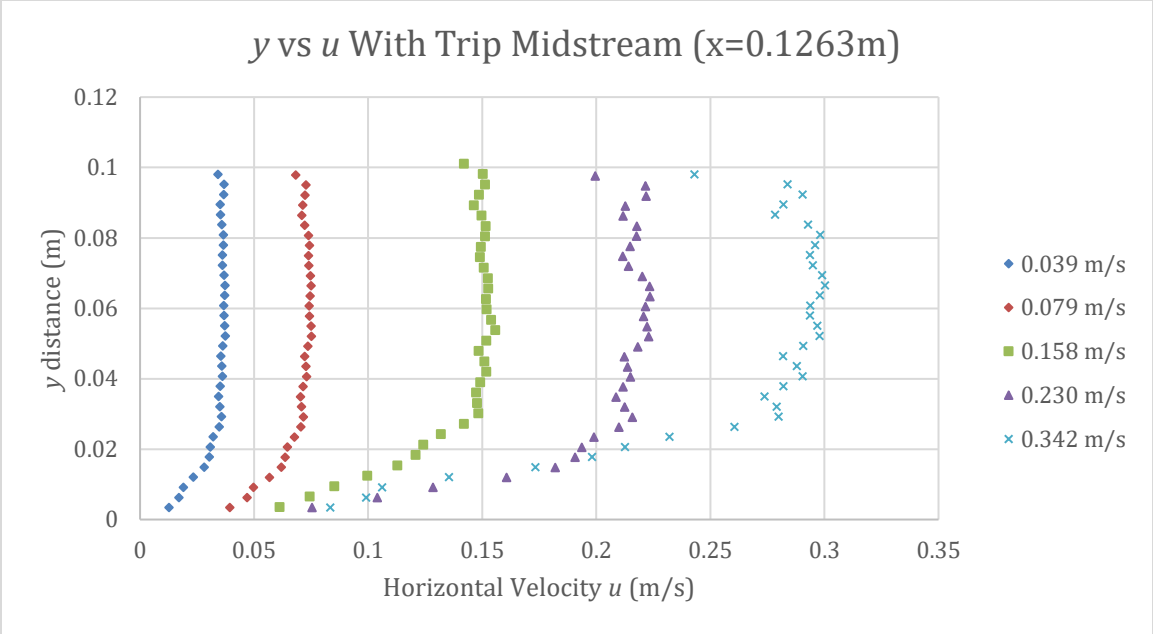


**Figure 24:** Horizontal velocity profile for midstream location of x=0.1263m with trip. Overall velocities are slower and exhibit greater ramp up to $U_\infty$ than previously.

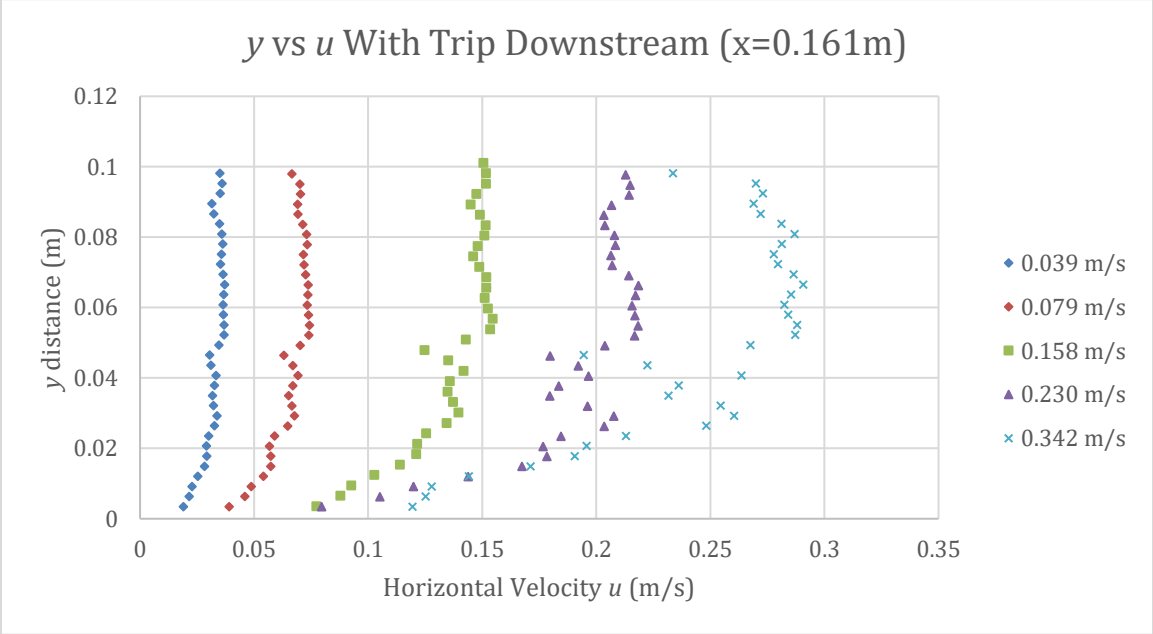


**Figure 25:** Horizontal velocity profile for downstream location at x=0.161m with trip. Greatest breakdown in horizontal velocity consistency at higher freestream speeds.

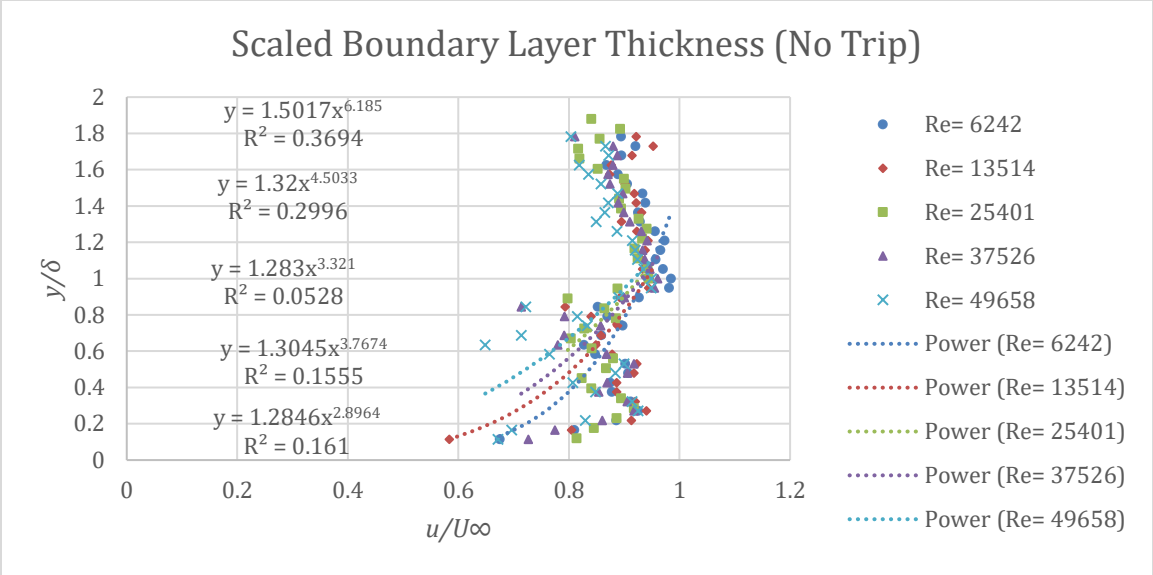


**Figure 26:** Non-dimensionalized scaled boundary layer thickness for all 5 freestream speeds for the no trip condition. Test conditions applied include the most downstream location of 0.1597-0.165m which vary due to the PIVlab analysis. The kinematic viscosity of water was applied for 21°C which equaled 9.757e-7 $m^2/s$. The described freestream speeds were used in the Reynolds number calculations. They Reynolds numbers are used in the legend. Further elaboration on the power curves in given in Table 4.

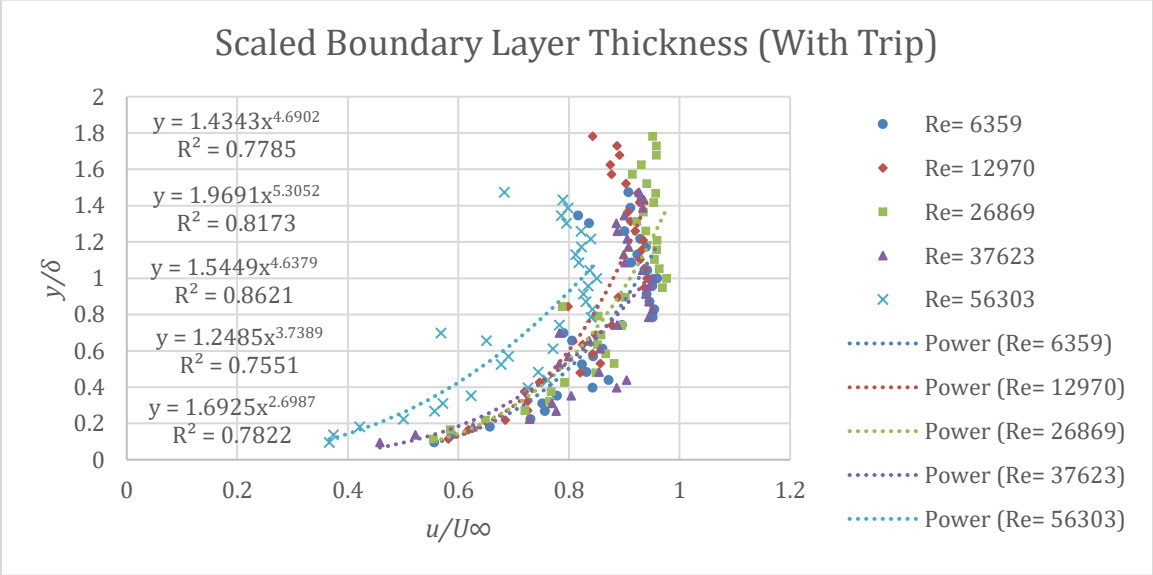


**Figure 27:** Non-dimensionalized scaled boundary layer thickness for all 5 freestream speeds for the trip condition. Test conditions applied include the most downstream location of 0.1599-0.1655m which vary due to the PIVlab analysis. The kinematic viscosity of water was applied for 21°C which equaled 9.757e-7 $m^2/s$. The described freestream speeds were used in the Reynolds number calculations. They Reynolds numbers are used in the legend. Further elaboration on the power curves in given in Table 4.

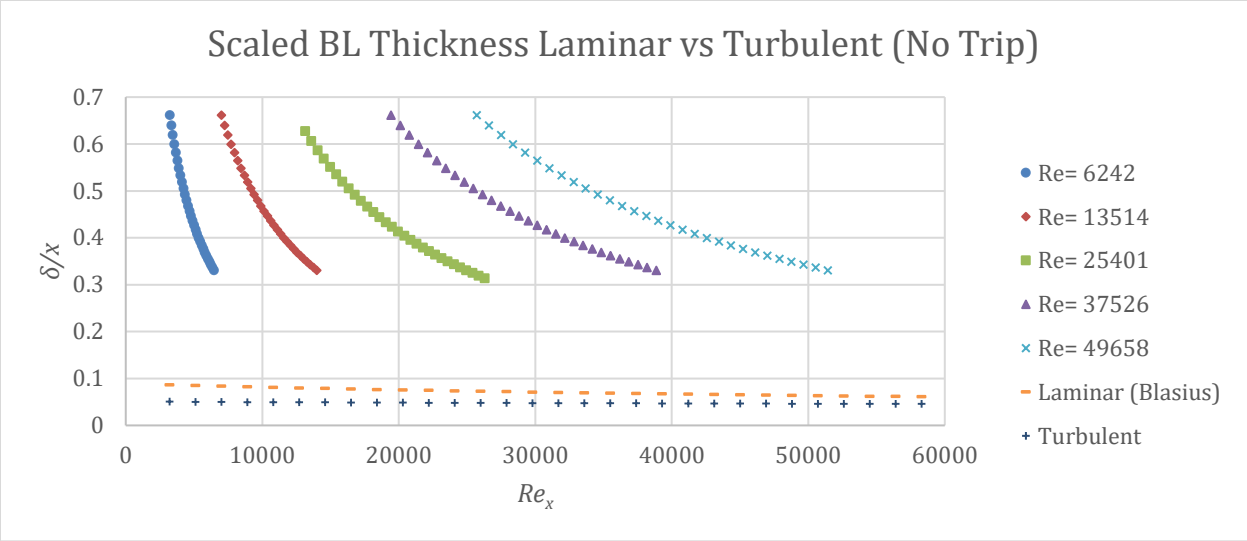


**Figure 28**: Non-dimensional boundary layer thickness over x location vs localized Reynolds number for each freestream Reynolds number tested. The Blasius and turbulent solutions are also shown for comparison. The large discrepancies are due to the thick boundary layer stemming from the $U_\infty$ definition method selected and many u points not reaching 99% of the freestream velocity.

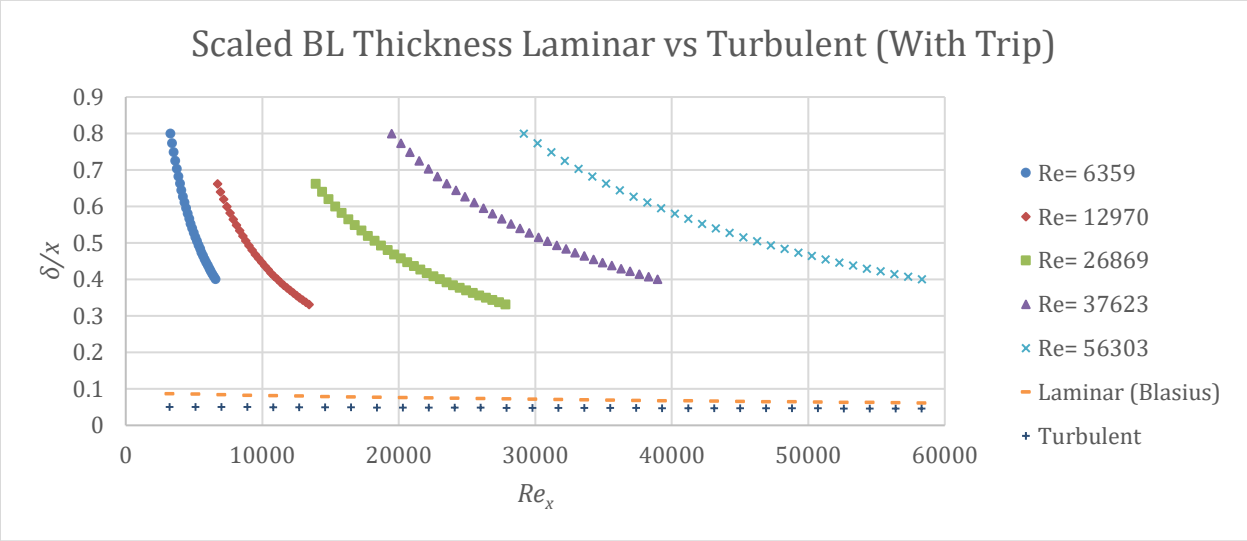


**Figure 29**: Non-dimensional boundary layer thickness over x location vs localized Reynolds number for each freestream Reynolds number tested with the trip condition. The large discrepancies from the Blasius and turbulent conditions are due to the thick boundary layer stemming from the $U_\infty$ definition method selected and many u points not reaching 99% of the freestream velocity. For a smaller boundary layer, the δ/x quantity is also reduced and more closely matches those approximations.

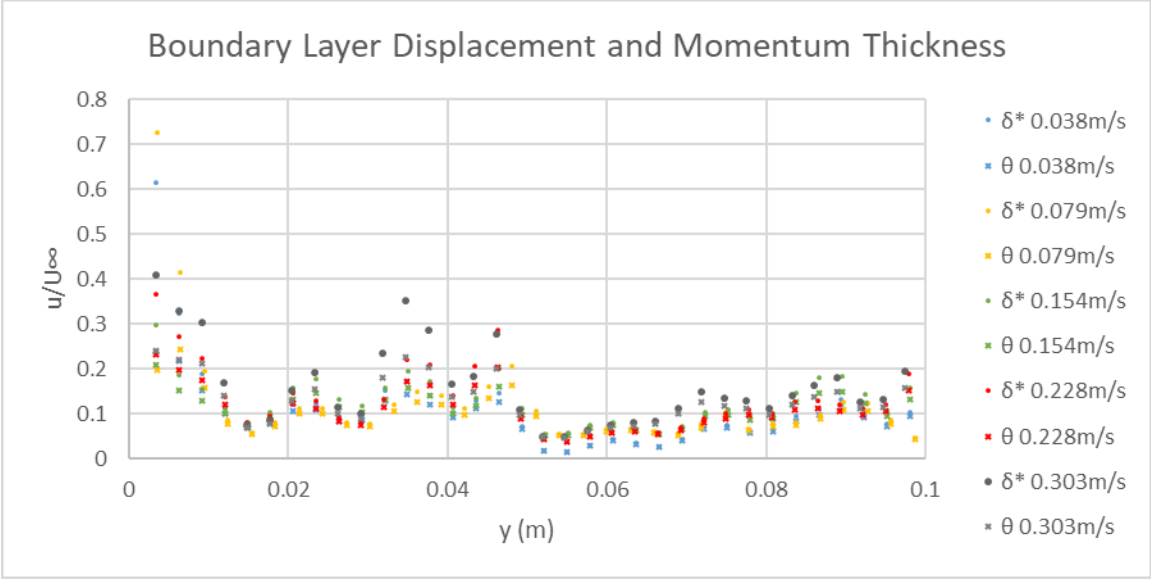


**Figure 30**: Calculation of displacement thickness and momentum thickness which are the area under their respective curves. These are match each other well.

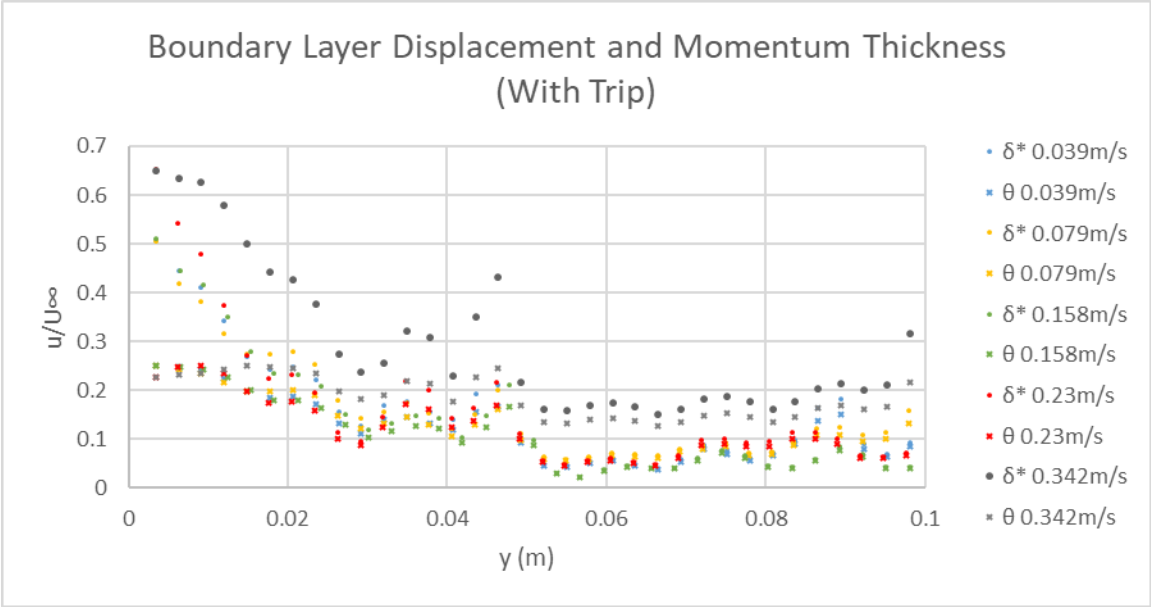


**Figure 31:** Calculation of displacement thickness and momentum thickness which are the area under their respective curves. These feature similar shape profiles but exhibit more variance than the no trip condition. There is greater fluctuation due to turbulence.

## APPENDIX

| | | U∞ | 0.0379 | m/s | | | Spec U∞ | 0.0435 | 0.0412 | m/s | | | | |
|---|---|---|---|---|---|---|---|---|---|---|---|---|---|---|
| es 1:499, conversion factor xy (px -> m): 0.0001793, conversion factor uv (px/frame -> m/s): 0.014344 | | | | | | | | | | | | | | |
| 99% U∞ | 0.037534 | m/s | 0.056561 | δ (m) | 99% U∞ | 0.037534 | m/s | 0.054653 | δ (m) | 99% U∞ | 0.037534 | m/s | 0.055044 | δ (m) |
| x1 | y1 | u1 | δ1 | v1 | x2 | y2 | u2 | δ2 | v2 | x3 | y3 | u3 | δ3 | v3 |
| 0.088931 | 0.098075 | 0.032588 | 0.090602 | -0.00194 | 0.126225 | 0.098075 | 0.030116 | 0.093253 | -0.00242 | 0.160650 | 0.098075 | 0.03391 | 0.087527 | -0.00306 |
| 0.088931 | 0.095207 | 0.034487 | 0.072616 | -0.00312 | 0.126225 | 0.095207 | 0.034529 | 0.079685 | -0.00358 | 0.160650 | 0.095207 | 0.034895 | 0.103122 | -0.00391 |
| 0.088931 | 0.092338 | 0.034874 | 0.114876 | -0.00349 | 0.126225 | 0.092338 | 0.035084 | 0.098443 | -0.00302 | 0.160650 | 0.092338 | 0.033939 | 0.102171 | -0.00274 |
| 0.088931 | 0.089469 | 0.034535 | 0.078257 | -0.00264 | 0.126225 | 0.089469 | 0.033933 | 0.045233 | -0.00219 | 0.160650 | 0.089469 | 0.03289 | 0.072827 | -0.00199 |
| 0.088931 | 0.0866 | 0.035303 | 0.079859 | -0.00271 | 0.126225 | 0.0866 | 0.034167 | 0.078796 | -0.0022 | 0.160650 | 0.0866 | 0.033691 | 0.069485 | -0.00221 |
| 0.088931 | 0.083732 | 0.036252 | 0.078398 | -0.00306 | 0.126225 | 0.083732 | 0.035405 | 0.075187 | -0.00272 | 0.160650 | 0.083732 | 0.034335 | 0.074981 | -0.00276 |
| 0.088931 | 0.080863 | 0.036942 | -0.07709 | -0.00331 | 0.126225 | 0.080863 | 0.03612 | 0.015408 | -0.00283 | 0.160650 | 0.080863 | 0.035384 | 0.049444 | -0.00295 |
| 0.088931 | 0.077994 | 0.036953 | 0.085686 | -0.00275 | 0.126225 | 0.077994 | 0.036182 | 0.088423 | -0.0024 | 0.160650 | 0.077994 | 0.03558 | 0.089105 | -0.00231 |
| 0.088931 | 0.075125 | 0.036736 | -0.25101 | -0.0023 | 0.126225 | 0.075125 | 0.03581 | -0.24693 | -0.00212 | 0.160650 | 0.075125 | 0.035076 | 0.023097 | -0.00184 |
| 0.088931 | 0.072257 | 0.036743 | 0.066575 | -0.00204 | 0.126225 | 0.072257 | 0.035825 | 0.065835 | -0.00202 | 0.160650 | 0.072257 | 0.035211 | 0.065807 | -0.00195 |
| 0.088931 | 0.069388 | 0.037142 | 0.063847 | -0.00182 | 0.126225 | 0.069388 | 0.036589 | 0.064442 | -0.00213 | 0.160650 | 0.069388 | 0.036244 | 0.063716 | -0.00207 |
| 0.088931 | 0.066519 | 0.037345 | 0.070481 | -0.00156 | 0.126225 | 0.066519 | 0.037137 | 0.111422 | -0.00181 | 0.160650 | 0.066519 | 0.036897 | 0.072764 | -0.00161 |
| 0.088931 | 0.06365 | 0.037208 | 0.087878 | -0.00093 | 0.126225 | 0.06365 | 0.037112 | 0.066803 | -0.00132 | 0.160650 | 0.06365 | 0.036604 | 0.071926 | -0.00089 |
| 0.088931 | 0.060782 | 0.03717 | 0.056496 | -0.00031 | 0.126225 | 0.060782 | 0.036727 | 0.039845 | -0.00087 | 0.160650 | 0.060782 | 0.036282 | 0.053634 | -0.00046 |
| 0.088931 | 0.057913 | 0.037414 | 0.056561 | 0.000237 | 0.126225 | 0.057913 | 0.036838 | 0.054908 | -0.00056 | 0.160650 | 0.057913 | 0.036784 | 0.053934 | -0.00026 |
| 0.088931 | 0.055044 | 0.037670 | 0.058502 | 0.000788 | 0.126225 | 0.055044 | 0.037503 | 0.054653 | -0.0001 | 0.160650 | 0.055044 | 0.037325 | 0.059805 | 0.000213 |
| 0.088931 | 0.052175 | 0.037782 | 0.048187 | 0.001289 | 0.126225 | 0.052175 | 0.037735 | 0.051621 | 0.000647 | 0.160650 | 0.052175 | 0.037199 | 0.052641 | 0.000974 |
| 0.088931 | 0.049307 | 0.037604 | 0.04875 | 0.001544 | 0.126225 | 0.049307 | 0.036698 | 0.0522 | 0.000865 | 0.160650 | 0.049307 | 0.035132 | 0.051738 | 0.000858 |
| 0.088931 | 0.046438 | 0.037245 | 0.039229 | 0.001706 | 0.126225 | 0.046438 | 0.03587 | 0.034997 | 0.00099 | 0.160650 | 0.046438 | 0.032297 | 0.024143 | 0.000728 |
| 0.088931 | 0.043569 | 0.03736 | 0.028403 | 0.001981 | 0.126225 | 0.043569 | 0.036287 | -0.26127 | 0.00129 | 0.160650 | 0.043569 | 0.032971 | 0.030992 | 0.000893 |
| 0.088931 | 0.0407 | 0.037393 | 0.0414 | 0.002008 | 0.126225 | 0.0407 | 0.036299 | 0.043988 | 0.001422 | 0.160650 | 0.0407 | 0.034012 | 0.047581 | 0.000792 |
| 0.088931 | 0.037832 | 0.036815 | 0.042216 | 0.00168 | 0.126225 | 0.037832 | 0.035221 | 0.051671 | 0.001225 | 0.160650 | 0.037832 | 0.032543 | 0.049992 | 0.000569 |
| 0.088931 | 0.034963 | 0.036344 | 0.134537 | 0.001335 | 0.126225 | 0.034963 | 0.034741 | 0.020695 | 0.000979 | 0.160650 | 0.034963 | 0.031365 | 0.012174 | 0.000391 |
| 0.088931 | 0.032094 | 0.03631 | 0.021902 | 0.001156 | 0.126225 | 0.032094 | 0.035303 | 0.023888 | 0.000859 | 0.160650 | 0.032094 | 0.032142 | 0.024593 | 0.000345 |
| 0.088931 | 0.029225 | 0.036654 | 0.036631 | 0.000989 | 0.126225 | 0.029225 | 0.036083 | 0.052584 | 0.000718 | 0.160650 | 0.029225 | 0.034204 | -0.02064 | 0.000247 |
| 0.088931 | 0.026357 | 0.036313 | 0.030573 | 0.000578 | 0.126225 | 0.026357 | 0.035905 | 0.031332 | 0.000353 | 0.160650 | 0.026357 | 0.034396 | 0.033657 | -5E-05 |
| 0.088931 | 0.023488 | 0.035483 | 0.043592 | 0.00027 | 0.126225 | 0.023488 | 0.034965 | 0.087851 | 0.000112 | 0.160650 | 0.023488 | 0.033162 | -0.09288 | -0.00026 |
| 0.088931 | 0.020619 | 0.03519 | 0.002933 | 0.000193 | 0.126225 | 0.020619 | 0.034851 | 0.012583 | 7.5E-06 | 0.160650 | 0.020619 | 0.03327 | 0.011266 | -0.0003 |
| 0.088931 | 0.01775 | 0.03557 | 0.00511 | 0.00012 | 0.126225 | 0.01775 | 0.035809 | 0.005044 | -0.00014 | 0.160650 | 0.01775 | 0.034578 | 0.001448 | -0.00045 |
| 0.088931 | 0.014882 | 0.036016 | 0.016988 | -5.3E-05 | 0.126225 | 0.014882 | 0.036198 | 0.017027 | -0.00035 | 0.160650 | 0.014882 | 0.035098 | 0.019486 | -0.0007 |
| 0.088931 | 0.012013 | 0.033948 | 0.014257 | -0.0003 | 0.126225 | 0.012013 | 0.034412 | 0.014254 | -0.00047 | 0.160650 | 0.012013 | 0.03358 | 0.015955 | -0.00075 |
| 0.088931 | 0.009144 | 0.029364 | 0.015096 | -0.00019 | 0.126225 | 0.009144 | 0.030415 | 0.014046 | -0.0004 | 0.160650 | 0.009144 | 0.030703 | 0.01298 | -0.00063 |
| 0.088931 | 0.006275 | 0.025426 | 0.010311 | -0.00011 | 0.126225 | 0.006275 | 0.026248 | 0.009478 | -0.00018 | 0.160650 | 0.006275 | 0.025593 | 0.009401 | -0.00038 |
| 0.088931 | 0.003407 | 0.01682 | 0.007602 | -8E-05 | 0.126225 | 0.003407 | 0.01614 | 0.007923 | -0.00022 | 0.160650 | 0.003407 | 0.014633 | 0.008738 | -0.00038 |

Raw Data of 3 x-locations for 50Hz No Trip.

| | | U∞ | 0.07920 | m/s | | | Spec U∞ | | 0.0857 | 0.0808 | m/s | | | |
|---|---|---|---|---|---|---|---|---|---|---|---|---|---|---|
| es 1:499, conversion factor xy (px -> m): 0.00018581, conversion factor uv (px/frame -> m/s): 0.027858 | | | | | | | | | | | | | | |
| 99% U∞ | 0.078408 | m/s | 0.068936 | δ (m) | 99% U∞ | 0.078408 | m/s | 0.054071 | δ (m) | 99% U∞ | 0.078408 | m/s | 0.057044 | δ (m) |
| x1 | y1 | u1 | δ1 | v1 | x2 | y2 | u2 | δ2 | v2 | x3 | y3 | u3 | δ3 | v3 |
| 0.092162 | 0.101639 | 0.068135 | 0.094387 | -0.00484 | 0.130811 | 0.101639 | 0.064667 | 0.097707 | -0.00647 | 0.166486 | 0.101639 | 0.07298 | 0.095003 | -0.00908 |
| 0.092162 | 0.098666 | 0.072347 | 0.092144 | -0.01104 | 0.130811 | 0.098666 | 0.075057 | 0.245213 | -0.01136 | 0.166486 | 0.098666 | 0.075412 | 0.101609 | -0.00925 |
| 0.092162 | 0.095693 | 0.07511 | 0.129132 | -0.01101 | 0.130811 | 0.095693 | 0.074989 | 0.101571 | -0.01053 | 0.166486 | 0.095693 | 0.072385 | 0.101698 | -0.00867 |
| 0.092162 | 0.09272 | 0.074816 | 0.080924 | -0.00958 | 0.130811 | 0.09272 | 0.07326 | 0.203958 | -0.00902 | 0.166486 | 0.09272 | 0.069404 | 0.218427 | -0.00601 |
| 0.092162 | 0.089747 | 0.075722 | 0.083132 | -0.01046 | 0.130811 | 0.089747 | 0.073122 | 0.078245 | -0.00908 | 0.166486 | 0.089747 | 0.069191 | 0.077244 | -0.00719 |
| 0.092162 | 0.086774 | 0.076929 | 0.081197 | -0.01183 | 0.130811 | 0.086774 | 0.074488 | 0.075336 | -0.01045 | 0.166486 | 0.086774 | 0.071382 | 0.071346 | -0.00889 |
| 0.092162 | 0.083801 | 0.077718 | 5.09244 | -0.01264 | 0.130811 | 0.083801 | 0.075507 | 0.118018 | -0.01098 | 0.166486 | 0.083801 | 0.072736 | 0.017101 | -0.00896 |
| 0.092162 | 0.080828 | 0.077717 | 0.087234 | -0.01153 | 0.130811 | 0.080828 | 0.075255 | 0.089115 | -0.00956 | 0.166486 | 0.080828 | 0.072989 | 0.06041 | -0.00769 |
| 0.092162 | 0.077855 | 0.077396 | 0.107064 | -0.01047 | 0.130811 | 0.077855 | 0.074124 | 0.021535 | -0.00873 | 0.166486 | 0.077855 | 0.073778 | 0.08259 | -0.00644 |
| 0.092162 | 0.074882 | 0.077293 | 0.069539 | -0.01044 | 0.130811 | 0.074882 | 0.07435 | 0.065441 | -0.00907 | 0.166486 | 0.074882 | 0.070871 | 0.06477 | -0.00771 |
| 0.092162 | 0.071909 | 0.077914 | 0.067167 | -0.01114 | 0.130811 | 0.071909 | 0.075628 | 0.058651 | -0.01021 | 0.166486 | 0.071909 | 0.073087 | 0.061894 | -0.00919 |
| 0.092162 | 0.068936 | 0.078224 | 0.072497 | -0.01137 | 0.130811 | 0.068936 | 0.076251 | 0.087746 | -0.01009 | 0.166486 | 0.068936 | 0.074667 | 0.096427 | -0.00921 |
| 0.092162 | 0.065963 | 0.07807 | 0.077558 | -0.01048 | 0.130811 | 0.065963 | 0.075911 | 0.075894 | -0.00907 | 0.166486 | 0.065963 | 0.074262 | 0.092132 | -0.00808 |
| 0.092162 | 0.06299 | 0.077983 | 0.135999 | -0.0099 | 0.130811 | 0.06299 | 0.075163 | 1.224165 | -0.00868 | 0.166486 | 0.06299 | 0.073791 | -0.0731 | -0.00757 |
| 0.092162 | 0.060017 | 0.077966 | 0.035826 | -0.00982 | 0.130811 | 0.060017 | 0.075155 | 0.046503 | -0.00876 | 0.166486 | 0.060017 | 0.073892 | 0.046017 | -0.00776 |
| 0.092162 | 0.057044 | 0.078020 | 0.063376 | -0.00946 | 0.130811 | 0.057044 | 0.07587 | 0.038292 | -0.00873 | 0.166486 | 0.057044 | 0.074851 | 0.176869 | -0.00773 |
| 0.092162 | 0.054071 | 0.077838 | 0.05735 | -0.00847 | 0.130811 | 0.054071 | 0.076273 | 0.057893 | -0.00758 | 0.166486 | 0.054071 | 0.074763 | 0.056699 | -0.00616 |
| 0.092162 | 0.051098 | 0.077321 | 0.055804 | -0.00647 | 0.130811 | 0.051098 | 0.074612 | 0.059161 | -0.00548 | 0.166486 | 0.051098 | 0.070639 | 0.054047 | -0.0038 |
| 0.092162 | 0.048125 | 0.076634 | 0.003218 | -0.00472 | 0.130811 | 0.048125 | 0.073212 | 0.033216 | -0.00386 | 0.166486 | 0.048125 | 0.062807 | 0.035688 | -0.00241 |
| 0.092162 | 0.045152 | 0.076751 | -0.00502 | -0.00363 | 0.130811 | 0.045152 | 0.074248 | 0.008504 | -0.00315 | 0.166486 | 0.045152 | 0.066536 | 0.03582 | -0.00184 |
| 0.092162 | 0.042179 | 0.07685 | 0.047625 | -0.00284 | 0.130811 | 0.042179 | 0.074586 | 0.049941 | -0.00251 | 0.166486 | 0.042179 | 0.070319 | 0.052343 | -0.0021 |
| 0.092162 | 0.039206 | 0.075999 | 0.048351 | -0.00174 | 0.130811 | 0.039206 | 0.073122 | 0.071204 | -0.00153 | 0.166486 | 0.039206 | 0.067952 | 0.082313 | -0.00139 |
| 0.092162 | 0.036233 | 0.075216 | -0.50669 | -0.00048 | 0.130811 | 0.036233 | 0.07263 | 0.024346 | -0.00035 | 0.166486 | 0.036233 | 0.067231 | 0.021996 | -0.00045 |
| 0.092162 | 0.03326 | 0.075233 | 0.018652 | 0.000477 | 0.130811 | 0.03326 | 0.074075 | 0.02275 | 0.000531 | 0.166486 | 0.03326 | 0.069565 | 0.025764 | 0.000283 |
| 0.092162 | 0.030287 | 0.075879 | 0.043665 | 0.001068 | 0.130811 | 0.030287 | 0.075301 | 0.044786 | 0.001136 | 0.166486 | 0.030287 | 0.073072 | 0.068782 | 0.000878 |
| 0.092162 | 0.027314 | 0.075317 | 0.034536 | 0.001097 | 0.130811 | 0.027314 | 0.074664 | 0.034309 | 0.001306 | 0.166486 | 0.027314 | 0.07266 | 0.034209 | 0.001087 |
| 0.092162 | 0.024341 | 0.074045 | 0.045132 | 0.0011 | 0.130811 | 0.024341 | 0.073072 | -0.09013 | 0.001435 | 0.166486 | 0.024341 | 0.070182 | -0.73875 | 0.00095 |
| 0.092162 | 0.021368 | 0.073421 | 0.009543 | 0.001264 | 0.130811 | 0.021368 | 0.073211 | 0.010675 | 0.001533 | 0.166486 | 0.021368 | 0.070214 | 0.012178 | 0.0011 |
| 0.092162 | 0.018395 | 0.074675 | 0.010033 | 0.001326 | 0.130811 | 0.018395 | 0.074656 | 0.009536 | 0.001529 | 0.166486 | 0.018395 | 0.072864 | 0.008038 | 0.001202 |
| 0.092162 | 0.015422 | 0.076002 | 0.018609 | 0.001006 | 0.130811 | 0.015422 | 0.075915 | 0.020122 | 0.001169 | 0.166486 | 0.015422 | 0.074456 | 0.020938 | 0.000964 |
| 0.092162 | 0.012449 | 0.073757 | 0.013821 | 0.00032 | 0.130811 | 0.012449 | 0.074338 | 0.014013 | 0.000596 | 0.166486 | 0.012449 | 0.072326 | 0.014548 | 0.000621 |
| 0.092162 | 0.009476 | 0.06368 | 0.013598 | -0.00033 | 0.130811 | 0.009476 | 0.066598 | 0.011675 | 0.000199 | 0.166486 | 0.009476 | 0.063707 | 0.011972 | 0.000294 |
| 0.092162 | 0.006503 | 0.053056 | 0.010192 | 1.8E-05 | 0.130811 | 0.006503 | 0.050627 | 0.00929 | -3.7E-05 | 0.166486 | 0.006503 | 0.046196 | 0.01041 | -0.00021 |
| 0.092162 | 0.00353 | 0.032624 | 0.008485 | -1.1E-05 | 0.130811 | 0.00353 | 0.020984 | 0.013191 | -0.00083 | 0.166486 | 0.00353 | 0.02168 | 0.012768 | -0.00151 |

Raw Data of 3 x-locations for 10Hz No Trip.

| | | U∞ | 0.154 | m/s | | Spec U∞ | 0.1686 | 0.1585 | m/s | | | | | |
|---|---|---|---|---|---|---|---|---|---|---|---|---|---|---|
| es 1:499, conversion factor xy (px -> m): 0.0001794, conversion factor uv (px/frame -> m/s): 0.053875 | | | | | | | | | | | | | | |
| 99% U∞ | 0.152637 | m/s | 0.066559 | δ (m) | 99% U∞ | 0.152637 | m/s | 0.066559 | δ (m) | 99% U∞ | 0.152637 | m/s | 0.052206 | δ (m) |
| x1 | y1 | u1 | δ1 | v1 | x2 | y2 | u2 | δ2 | v2 | x3 | y3 | u3 | δ3 | v3 |
| 0.088984 | 0.098134 | 0.117711 | 0.09352 | -0.00493 | 0.1263 | 0.098134 | 0.115037 | 0.093489 | -0.00831 | 0.160746 | 0.098134 | 0.129567 | 0.089907 | -0.01743 |
| 0.088984 | 0.095263 | 0.139439 | 0.081536 | -0.01212 | 0.1263 | 0.095263 | 0.138276 | 0.597128 | -0.01401 | 0.160746 | 0.095263 | 0.137617 | 0.10285 | -0.01699 |
| 0.088984 | 0.092393 | 0.142199 | 0.097427 | -0.01282 | 0.1263 | 0.092393 | 0.138193 | 0.098405 | -0.01223 | 0.160746 | 0.092393 | 0.131934 | 0.102273 | -0.01065 |
| 0.088984 | 0.089522 | 0.136247 | 0.079429 | -0.01188 | 0.1263 | 0.089522 | 0.131298 | 0.046828 | -0.00957 | 0.160746 | 0.089522 | 0.125918 | -0.13076 | -0.00684 |
| 0.088984 | 0.086652 | 0.140908 | 0.077423 | -0.01138 | 0.1263 | 0.086652 | 0.132732 | 0.072791 | -0.00965 | 0.160746 | 0.086652 | 0.126267 | 0.07183 | -0.008 |
| 0.088984 | 0.083781 | 0.144556 | 0.07343 | -0.0139 | 0.1263 | 0.083781 | 0.136854 | 0.071102 | -0.01217 | 0.160746 | 0.083781 | 0.131374 | 0.075432 | -0.01121 |
| 0.088984 | 0.080911 | 0.146797 | 0.19458 | -0.01578 | 0.1263 | 0.080911 | 0.140428 | 0.035114 | -0.01324 | 0.160746 | 0.080911 | 0.138684 | -0.01341 | -0.01232 |
| 0.088984 | 0.078041 | 0.14665 | 0.107986 | -0.01408 | 0.1263 | 0.078041 | 0.141193 | 0.125492 | -0.01119 | 0.160746 | 0.078041 | 0.139109 | 0.099922 | -0.00917 |
| 0.088984 | 0.07517 | 0.146076 | 0.063538 | -0.01242 | 0.1263 | 0.07517 | 0.140501 | 0.058357 | -0.00979 | 0.160746 | 0.07517 | 0.137334 | -0.00179 | -0.00756 |
| 0.088984 | 0.0723 | 0.147695 | 0.067788 | -0.01281 | 0.1263 | 0.0723 | 0.142573 | 0.063419 | -0.01015 | 0.160746 | 0.0723 | 0.137905 | 0.063628 | -0.00852 |
| 0.088984 | 0.069429 | 0.150839 | 0.065755 | -0.01357 | 0.1263 | 0.069429 | 0.145826 | 0.056762 | -0.01175 | 0.160746 | 0.069429 | 0.142782 | 0.057115 | -0.0103 |
| 0.088984 | 0.066559 | 0.152244 | 0.069689 | -0.01328 | 0.1263 | 0.066559 | 0.147369 | 0.111717 | -0.01144 | 0.160746 | 0.066559 | 0.145079 | 0.083421 | -0.01006 |
| 0.088984 | 0.063688 | 0.151883 | 0.071138 | -0.01187 | 0.1263 | 0.063688 | 0.147034 | 0.073369 | -0.01031 | 0.160746 | 0.063688 | 0.143792 | 0.075757 | -0.00825 |
| 0.088984 | 0.060818 | 0.151593 | 0.054919 | -0.01113 | 0.1263 | 0.060818 | 0.145373 | 0.881637 | -0.01008 | 0.160746 | 0.060818 | 0.141689 | 0.023461 | -0.00807 |
| 0.088984 | 0.057947 | 0.152101 | 0.030479 | -0.01148 | 0.1263 | 0.057947 | 0.145348 | 0.044559 | -0.01089 | 0.160746 | 0.057947 | 0.14253 | 0.04754 | -0.0094 |
| 0.088984 | 0.055077 | 0.152157 | 0.056712 | -0.01178 | 0.1263 | 0.055077 | 0.146911 | 0.008557 | -0.01192 | 0.160746 | 0.055077 | 0.145317 | -0.03697 | -0.01054 |
| 0.088984 | 0.052206 | 0.151314 | 0.054702 | -0.01119 | 0.1263 | 0.052206 | 0.147264 | 0.056715 | -0.01125 | 0.160746 | 0.052206 | 0.145546 | 0.054566 | -0.00938 |
| 0.088984 | 0.049336 | 0.149793 | 0.053884 | -0.0094 | 0.1263 | 0.049336 | 0.143843 | 0.058853 | -0.00906 | 0.160746 | 0.049336 | 0.136919 | 0.052586 | -0.00677 |
| 0.088984 | 0.046466 | 0.147998 | 0.015923 | -0.00811 | 0.1263 | 0.046466 | 0.14119 | 0.033341 | -0.00784 | 0.160746 | 0.046466 | 0.123036 | 0.038118 | -0.00564 |
| 0.088984 | 0.043595 | 0.148434 | -0.01959 | -0.0081 | 0.1263 | 0.043595 | 0.143694 | 0.014774 | -0.00812 | 0.160746 | 0.043595 | 0.133215 | 0.026322 | -0.00633 |
| 0.088984 | 0.040725 | 0.148625 | 0.046011 | -0.00856 | 0.1263 | 0.040725 | 0.144584 | 0.047647 | -0.00903 | 0.160746 | 0.040725 | 0.136443 | 0.046008 | -0.00744 |
| 0.088984 | 0.037854 | 0.146446 | 0.044528 | -0.00775 | 0.1263 | 0.037854 | 0.141245 | 0.048655 | -0.00821 | 0.160746 | 0.037854 | 0.127644 | 0.057105 | -0.00698 |
| 0.088984 | 0.034984 | 0.143783 | 0.058596 | -0.00571 | 0.1263 | 0.034984 | 0.138218 | -0.05633 | -0.00644 | 0.160746 | 0.034984 | 0.123917 | 0.020603 | -0.00535 |
| 0.088984 | 0.032113 | 0.142707 | -0.04424 | -0.00517 | 0.1263 | 0.032113 | 0.138671 | 0.012536 | -0.00601 | 0.160746 | 0.032113 | 0.12965 | 0.0212 | -0.00525 |
| 0.088984 | 0.029243 | 0.14308 | 0.038388 | -0.00585 | 0.1263 | 0.029243 | 0.140719 | 0.044327 | -0.00671 | 0.160746 | 0.029243 | 0.135696 | 0.05335 | -0.00592 |
| 0.088984 | 0.026372 | 0.14008 | 0.031773 | -0.00593 | 0.1263 | 0.026372 | 0.138451 | 0.03415 | -0.00693 | 0.160746 | 0.026372 | 0.133679 | 0.034381 | -0.00592 |
| 0.088984 | 0.023502 | 0.133407 | 0.037999 | -0.00447 | 0.1263 | 0.023502 | 0.133215 | -0.01503 | -0.00519 | 0.160746 | 0.023502 | 0.126883 | -0.00352 | -0.00467 |
| 0.088984 | 0.020631 | 0.129599 | 0.011305 | -0.00283 | 0.1263 | 0.020631 | 0.134662 | 0.011475 | -0.00382 | 0.160746 | 0.020631 | 0.129619 | 0.012675 | -0.00384 |
| 0.088984 | 0.017761 | 0.13669 | 0.003619 | -0.00238 | 0.1263 | 0.017761 | 0.140297 | 0.005178 | -0.00379 | 0.160746 | 0.017761 | 0.137924 | 0.005802 | -0.00404 |
| 0.088984 | 0.01489 | 0.139926 | 0.022173 | -0.00314 | 0.1263 | 0.01489 | 0.143112 | 0.021574 | -0.00433 | 0.160746 | 0.01489 | 0.141455 | 0.021528 | -0.00419 |
| 0.088984 | 0.01202 | 0.134917 | 0.016266 | -0.00271 | 0.1263 | 0.01202 | 0.139021 | 0.017814 | -0.00377 | 0.160746 | 0.01202 | 0.13662 | 0.019267 | -0.00348 |
| 0.088984 | 0.00915 | 0.122937 | -0.00477 | -0.00216 | 0.1263 | 0.00915 | 0.132275 | -0.01001 | -0.00216 | 0.160746 | 0.00915 | 0.130275 | 0.022472 | -0.00266 |
| 0.088984 | 0.006279 | 0.129062 | 0.052498 | -0.00148 | 0.1263 | 0.006279 | 0.135326 | 0.01002 | -0.00171 | 0.160746 | 0.006279 | 0.125457 | 0.010806 | -0.00219 |
| 0.088984 | 0.003409 | 0.127598 | 0.004078 | -0.00102 | 0.1263 | 0.003409 | 0.122042 | 0.004263 | -0.00057 | 0.160746 | 0.003409 | 0.108223 | 0.004808 | -0.00206 |

Raw Data of 3 x-locations for 20Hz No Trip.

| | | U∞ | 0.228 | m/s | | Spec U∞ | 0.2501 | 0.2346 | m/s | | | | | |
|---|---|---|---|---|---|---|---|---|---|---|---|---|---|---|
| es 1:499, conversion factor xy (px -> m): 0.00017898, conversion factor uv (px/frame -> m/s): 0.071591 | | | | | | | | | | | | | | |
| 99% U∞ | 0.226034 | m/s | 0.055957 | δ (m) | 99% U∞ | 0.226034 | m/s | 0.052083 | δ (m) | 99% U∞ | 0.226034 | m/s | 0.054946 | δ (m) |
| x1 | y1 | u1 | δ1 | v1 | x2 | y2 | u2 | δ2 | v2 | x3 | y3 | u3 | δ3 | v3 |
| 0.088773 | 0.097901 | 0.189399 | 0.092874 | -0.01107 | 0.126001 | 0.097901 | 0.167971 | 0.093892 | -0.01025 | 0.160365 | 0.097901 | 0.185093 | 0.090481 | -0.01012 |
| 0.088773 | 0.095038 | 0.210268 | 0.14436 | -0.01903 | 0.126001 | 0.095038 | 0.209442 | 0.07719 | -0.01548 | 0.160365 | 0.095038 | 0.200893 | 0.053305 | -0.0148 |
| 0.088773 | 0.092174 | 0.209352 | 0.110914 | -0.01563 | 0.126001 | 0.092174 | 0.212104 | 0.096 | -0.01322 | 0.160365 | 0.092174 | 0.202618 | 0.129368 | -0.01248 |
| 0.088773 | 0.08931 | 0.206803 | 0.07872 | -0.01396 | 0.126001 | 0.08931 | 0.201679 | 0.007343 | -0.0091 | 0.160365 | 0.08931 | 0.200815 | 0.126112 | -0.01035 |
| 0.088773 | 0.086447 | 0.212003 | 0.079607 | -0.01108 | 0.126001 | 0.086447 | 0.20253 | 0.075415 | -0.01016 | 0.160365 | 0.086447 | 0.198852 | -0.01931 | -0.01051 |
| 0.088773 | 0.083583 | 0.217877 | 0.076136 | -0.01329 | 0.126001 | 0.083583 | 0.208631 | 0.070998 | -0.01174 | 0.160365 | 0.083583 | 0.199588 | 0.069335 | -0.01313 |
| 0.088773 | 0.080719 | 0.221014 | 0.064802 | -0.01435 | 0.126001 | 0.080719 | 0.212591 | 0.027895 | -0.01086 | 0.160365 | 0.080719 | 0.204904 | 0.112374 | -0.01077 |
| 0.088773 | 0.077856 | 0.221917 | 0.092048 | -0.01216 | 0.126001 | 0.077856 | 0.21332 | 0.094738 | -0.0082 | 0.160365 | 0.077856 | 0.202992 | 0.049467 | -0.00703 |
| 0.088773 | 0.074992 | 0.221086 | 0.028211 | -0.00983 | 0.126001 | 0.074992 | 0.211163 | 0.058364 | -0.00633 | 0.160365 | 0.074992 | 0.205317 | 0.050449 | -0.00731 |
| 0.088773 | 0.072128 | 0.221389 | 0.06634 | -0.0089 | 0.126001 | 0.072128 | 0.213724 | 0.063751 | -0.00621 | 0.160365 | 0.072128 | 0.207734 | 0.061212 | -0.00729 |
| 0.088773 | 0.069265 | 0.223687 | 0.063036 | -0.00833 | 0.126001 | 0.069265 | 0.217932 | 0.055646 | -0.00697 | 0.160365 | 0.069265 | 0.212535 | 0.053238 | -0.00807 |
| 0.088773 | 0.066401 | 0.224766 | 0.089813 | -0.00761 | 0.126001 | 0.066401 | 0.219636 | -0.23438 | -0.00663 | 0.160365 | 0.066401 | 0.214947 | 0.082777 | -0.00681 |
| 0.088773 | 0.063537 | 0.224611 | 0.048861 | -0.00678 | 0.126001 | 0.063537 | 0.219697 | 0.084764 | -0.00571 | 0.160365 | 0.063537 | 0.213008 | 0.02649 | -0.00464 |
| 0.088773 | 0.060674 | 0.224889 | 0.054865 | -0.00637 | 0.126001 | 0.060674 | 0.218842 | 0.031405 | -0.00552 | 0.160365 | 0.060674 | 0.214015 | 0.044639 | -0.00375 |
| 0.088773 | 0.05781 | 0.225453 | 0.055957 | -0.00679 | 0.126001 | 0.05781 | 0.219545 | 0.050499 | -0.00564 | 0.160365 | 0.05781 | 0.216161 | 0.048826 | -0.00337 |
| 0.088773 | 0.054946 | 0.226350 | 0.056072 | -0.0065 | 0.126001 | 0.054946 | 0.222087 | 0.047078 | -0.00551 | 0.160365 | 0.054946 | 0.219308 | 0.069126 | -0.00352 |
| 0.088773 | 0.052083 | 0.227156 | 0.050372 | -0.00567 | 0.126001 | 0.052083 | 0.223524 | 0.053408 | -0.00431 | 0.160365 | 0.052083 | 0.21795 | 0.053949 | -0.00155 |
| 0.088773 | 0.049219 | 0.225278 | 0.049881 | -0.00444 | 0.126001 | 0.049219 | 0.218099 | 0.053187 | -0.00325 | 0.160365 | 0.049219 | 0.205544 | 0.050595 | -0.00085 |
| 0.088773 | 0.046355 | 0.222007 | 0.020331 | -0.00376 | 0.126001 | 0.046355 | 0.212373 | 0.026347 | -0.00253 | 0.160365 | 0.046355 | 0.162912 | 0.03629 | -0.00102 |
| 0.088773 | 0.043492 | 0.22245 | 0.08666 | -0.00331 | 0.126001 | 0.043492 | 0.214328 | -0.06836 | -0.00285 | 0.160365 | 0.043492 | 0.18087 | 0.034795 | -0.00038 |
| 0.088773 | 0.040628 | 0.222213 | 0.043387 | -0.00366 | 0.126001 | 0.040628 | 0.214628 | 0.04669 | -0.00391 | 0.160365 | 0.040628 | 0.195741 | 0.046382 | -0.00259 |
| 0.088773 | 0.037764 | 0.218246 | 0.044725 | -0.00373 | 0.126001 | 0.037764 | 0.209239 | 0.058389 | -0.00402 | 0.160365 | 0.037764 | 0.180665 | 0.087047 | -0.00331 |
| 0.088773 | 0.034901 | 0.215042 | 0.013318 | -0.00261 | 0.126001 | 0.034901 | 0.206907 | 0.022813 | -0.00333 | 0.160365 | 0.034901 | 0.178029 | 0.028079 | -0.00271 |
| 0.088773 | 0.032037 | 0.2165 | 0.024773 | -0.00181 | 0.126001 | 0.032037 | 0.211438 | 0.024596 | -0.00349 | 0.160365 | 0.032037 | 0.198179 | 0.025006 | -0.00303 |
| 0.088773 | 0.029173 | 0.220258 | 0.035636 | -0.00229 | 0.126001 | 0.029173 | 0.217056 | 0.046817 | -0.00464 | 0.160365 | 0.029173 | 0.209524 | 0.046622 | -0.004 |
| 0.088773 | 0.02631 | 0.217699 | 0.029809 | -0.0032 | 0.126001 | 0.02631 | 0.215598 | 0.031374 | -0.00554 | 0.160365 | 0.02631 | 0.206814 | 0.032859 | -0.00488 |
| 0.088773 | 0.023446 | 0.210878 | 0.037487 | -0.00259 | 0.126001 | 0.023446 | 0.209697 | 0.063721 | -0.00422 | 0.160365 | 0.023446 | 0.19841 | 0.046103 | -0.00444 |
| 0.088773 | 0.020583 | 0.207787 | -1.23446 | -0.00113 | 0.126001 | 0.020583 | 0.208536 | 0.011669 | -0.00292 | 0.160365 | 0.020583 | 0.194919 | 0.012991 | -0.00266 |
| 0.088773 | 0.017719 | 0.207829 | 0.007577 | -0.00062 | 0.126001 | 0.017719 | 0.214158 | 0.001041 | -0.00311 | 0.160365 | 0.017719 | 0.206656 | -0.00194 | -0.00343 |
| 0.088773 | 0.014855 | 0.212969 | 0.019054 | -0.00158 | 0.126001 | 0.014855 | 0.216197 | 0.017426 | -0.00423 | 0.160365 | 0.014855 | 0.209479 | 0.018491 | -0.00388 |
| 0.088773 | 0.011992 | 0.204059 | 0.013765 | -0.00229 | 0.126001 | 0.011992 | 0.205238 | 0.014789 | -0.00409 | 0.160365 | 0.011992 | 0.19644 | 0.016319 | -0.00351 |
| 0.088773 | 0.009128 | 0.168568 | 0.025158 | 0.000462 | 0.126001 | 0.009128 | 0.183951 | 0.021633 | -0.0029 | 0.160365 | 0.009128 | 0.176856 | 0.021901 | -0.00281 |
| 0.088773 | 0.006264 | 0.158303 | 0.020109 | -0.00075 | 0.126001 | 0.006264 | 0.174314 | 0.013484 | -0.00165 | 0.160365 | 0.006264 | 0.165831 | 0.014261 | -0.0026 |
| 0.088773 | 0.003401 | 0.144294 | 0.005327 | 0.000413 | 0.126001 | 0.003401 | 0.1538 | 0.004998 | -0.00042 | 0.160365 | 0.003401 | 0.144273 | 0.005328 | -0.00209 |

Raw Data of 3 x-locations for 30Hz No Trip.

| | | U∞ | 0.303 | m/s | | Spec U∞ | 0.3304 | 0.3095 | m/s | | | | | |
|---|---|---|---|---|---|---|---|---|---|---|---|---|---|---|
| es 1:499, conversion factor xy (px -> m): 0.00017825, conversion factor uv (px/frame -> m/s): 0.089124 | | | | | | | | | | | | | | |
| 99% U∞ | 0.300337 | m/s | 0.059604 | δ (m) | 99% U∞ | 0.300337 | m/s | 0.054722 | δ (m) | 99% U∞ | 0.300337 | m/s | 0.054722 | δ (m) |
| x1 | y1 | u1 | δ1 | v1 | x2 | y2 | u2 | δ2 | v2 | x3 | y3 | u3 | δ3 | v3 |
| 0.088411 | 0.097501 | 0.237314 | 0.092203 | -0.00464 | 0.125486 | 0.097501 | 0.244681 | 0.090597 | -0.0098 | 0.159709 | 0.097501 | 0.243838 | 0.088957 | -0.0122 |
| 0.088411 | 0.094649 | 0.271241 | -0.00739 | -0.00908 | 0.125486 | 0.094649 | 0.267672 | 0.076998 | -0.01324 | 0.159709 | 0.094649 | 0.262697 | 0.032508 | -0.01249 |
| 0.088411 | 0.091797 | 0.272054 | 0.098742 | -0.01043 | 0.125486 | 0.091797 | 0.27295 | 0.097638 | -0.01052 | 0.159709 | 0.091797 | 0.264424 | 0.098142 | -0.01023 |
| 0.088411 | 0.088945 | 0.260439 | 0.078969 | -0.00974 | 0.125486 | 0.088945 | 0.259576 | 0.074603 | -0.00654 | 0.159709 | 0.088945 | 0.24828 | 0.06021 | -0.00727 |
| 0.088411 | 0.086093 | 0.271844 | 0.078669 | -0.00765 | 0.125486 | 0.086093 | 0.267682 | 0.072718 | -0.00632 | 0.159709 | 0.086093 | 0.253447 | 0.066418 | -0.005 |
| 0.088411 | 0.083241 | 0.282789 | 0.07213 | -0.00759 | 0.125486 | 0.083241 | 0.274644 | 0.0691 | -0.00821 | 0.159709 | 0.083241 | 0.260244 | 0.070731 | -0.00818 |
| 0.088411 | 0.080389 | 0.287293 | 0.064352 | -0.00815 | 0.125486 | 0.080389 | 0.279826 | 0.04226 | -0.0078 | 0.159709 | 0.080389 | 0.269384 | 0.09766 | -0.00958 |
| 0.088411 | 0.077537 | 0.289613 | -0.55236 | -0.00628 | 0.125486 | 0.077537 | 0.28136 | 0.090008 | -0.00503 | 0.159709 | 0.077537 | 0.264272 | 0.129476 | -0.00723 |
| 0.088411 | 0.074686 | 0.289661 | 0.183702 | -0.00397 | 0.125486 | 0.074686 | 0.27702 | 0.039142 | -0.00457 | 0.159709 | 0.074686 | 0.262292 | 0.098423 | -0.00723 |
| 0.088411 | 0.071834 | 0.289382 | 0.06101 | -0.00342 | 0.125486 | 0.071834 | 0.278891 | 0.060863 | -0.00664 | 0.159709 | 0.071834 | 0.257721 | 0.061036 | -0.00946 |
| 0.088411 | 0.068982 | 0.292268 | 0.061774 | -0.00388 | 0.125486 | 0.068982 | 0.284466 | 0.059925 | -0.00915 | 0.159709 | 0.068982 | 0.268978 | 0.05848 | -0.0136 |
| 0.088411 | 0.06613 | 0.295461 | 0.061464 | -0.00511 | 0.125486 | 0.06613 | 0.289464 | 0.055884 | -0.00962 | 0.159709 | 0.06613 | 0.277494 | 0.026021 | -0.01209 |
| 0.088411 | 0.063278 | 0.298441 | 0.059409 | -0.00544 | 0.125486 | 0.063278 | 0.292491 | 0.043713 | -0.00842 | 0.159709 | 0.063278 | 0.279118 | 0.014568 | -0.01019 |
| 0.088411 | 0.060426 | 0.299839 | 0.059604 | -0.0057 | 0.125486 | 0.060426 | 0.293634 | 0.054457 | -0.00861 | 0.159709 | 0.060426 | 0.280361 | 0.044211 | -0.00979 |
| 0.088411 | 0.057574 | 0.301567 | 0.06242 | -0.00636 | 0.125486 | 0.057574 | 0.296837 | 0.050288 | -0.01027 | 0.159709 | 0.057574 | 0.283874 | 0.046013 | -0.01199 |
| 0.088411 | 0.054722 | 0.302291 | 0.043756 | -0.00704 | 0.125486 | 0.054722 | 0.298207 | 0.072816 | -0.01147 | 0.159709 | 0.054722 | 0.287936 | 0.368574 | -0.0128 |
| 0.088411 | 0.05187 | 0.301783 | 0.049804 | -0.00645 | 0.125486 | 0.05187 | 0.297871 | 0.053023 | -0.01015 | 0.159709 | 0.05187 | 0.287823 | 0.053894 | -0.01086 |
| 0.088411 | 0.049018 | 0.299786 | 0.049655 | -0.00502 | 0.125486 | 0.049018 | 0.291773 | 0.052029 | -0.00787 | 0.159709 | 0.049018 | 0.270188 | 0.050698 | -0.00778 |
| 0.088411 | 0.046166 | 0.297321 | 0.040001 | -0.00362 | 0.125486 | 0.046166 | 0.283662 | 0.020691 | -0.00708 | 0.159709 | 0.046166 | 0.219018 | 0.037971 | -0.0053 |
| 0.088411 | 0.043314 | 0.298716 | 0.101218 | -0.00333 | 0.125486 | 0.043314 | 0.285529 | 0.084082 | -0.00731 | 0.159709 | 0.043314 | 0.247318 | 0.015758 | -0.00646 |
| 0.088411 | 0.040462 | 0.298637 | 0.041227 | -0.00419 | 0.125486 | 0.040462 | 0.284493 | 0.045154 | -0.00782 | 0.159709 | 0.040462 | 0.252805 | 0.044193 | -0.00675 |
| 0.088411 | 0.03761 | 0.2923 | 0.042238 | -0.00365 | 0.125486 | 0.03761 | 0.274861 | 0.059514 | -0.0068 | 0.159709 | 0.03761 | 0.216469 | 0.049734 | -0.00513 |
| 0.088411 | 0.034758 | 0.287348 | -29.3098 | -0.00188 | 0.125486 | 0.034758 | 0.271544 | 0.024354 | -0.0056 | 0.159709 | 0.034758 | 0.19674 | 0.026386 | -0.006 |
| 0.088411 | 0.031906 | 0.287349 | 0.02211 | -0.00029 | 0.125486 | 0.031906 | 0.279437 | 0.024474 | -0.00532 | 0.159709 | 0.031906 | 0.232031 | 0.027152 | -0.00593 |
| 0.088411 | 0.029054 | 0.29113 | 0.034313 | -0.00027 | 0.125486 | 0.029054 | 0.287457 | 0.057946 | -0.00442 | 0.159709 | 0.029054 | 0.273003 | 0.045106 | -0.00727 |
| 0.088411 | 0.026202 | 0.286136 | 0.030234 | -0.00206 | 0.125486 | 0.026202 | 0.286186 | 0.030585 | -0.0056 | 0.159709 | 0.026202 | 0.268147 | 0.030131 | -0.00905 |
| 0.088411 | 0.02335 | 0.27609 | 0.033299 | -0.0025 | 0.125486 | 0.02335 | 0.276976 | -0.00439 | -0.00544 | 0.159709 | 0.02335 | 0.244778 | 0.010688 | -0.00651 |
| 0.088411 | 0.020498 | 0.26914 | -0.0324 | 9.76E-05 | 0.125486 | 0.020498 | 0.279378 | 0.013248 | -0.00494 | 0.159709 | 0.020498 | 0.257292 | 0.014387 | -0.00588 |
| 0.088411 | 0.017646 | 0.270822 | 0.011268 | -0.00081 | 0.125486 | 0.017646 | 0.287622 | 0.004167 | -0.0042 | 0.159709 | 0.017646 | 0.277378 | -0.00286 | -0.00617 |
| 0.088411 | 0.014795 | 0.284018 | 0.017327 | -0.00248 | 0.125486 | 0.014795 | 0.290312 | 0.016348 | -0.00626 | 0.159709 | 0.014795 | 0.280571 | 0.016741 | -0.00743 |
| 0.088411 | 0.011943 | 0.265638 | 0.014833 | -0.00112 | 0.125486 | 0.011943 | 0.271913 | 0.014794 | -0.0059 | 0.159709 | 0.011943 | 0.251604 | 0.015393 | -0.00432 |
| 0.088411 | 0.009091 | 0.231406 | 0.128515 | -0.00197 | 0.125486 | 0.009091 | 0.243488 | 0.015081 | -0.00452 | 0.159709 | 0.009091 | 0.211321 | 0.042494 | -0.00614 |
| 0.088411 | 0.006239 | 0.229759 | 0.012807 | -0.0012 | 0.125486 | 0.006239 | 0.216422 | 0.015456 | -0.0044 | 0.159709 | 0.006239 | 0.203721 | 0.017531 | -0.00549 |
| 0.088411 | 0.003387 | 0.199116 | 0.005108 | 0.00081 | 0.125486 | 0.003387 | 0.190459 | 0.005341 | -0.00517 | 0.159709 | 0.003387 | 0.179321 | 0.005672 | -0.00429 |

Raw Data of 3 x-locations for 40Hz No Trip.

| | | U∞ | 0.039 | m/s | | Spec U∞ | 0.0435 | 0.0412 | m/s | | | | | |
|---|---|---|---|---|---|---|---|---|---|---|---|---|---|---|
| es 1:499, conversion factor xy (px -> m): 0.0001793, conversion factor uv (px/frame -> m/s): 0.014344 | | | | | | | | | | | | | | |
| 99% U∞ | 0.038235 | m/s | 0.077994 | δ (m) | 99% U∞ | 0.038235 | m/s | 0.052175 | δ (m) | 99% U∞ | 0.038235 | m/s | 0.066519 | δ (m) |
| x1 | y1 | u1 | δ1 | v1 | x2 | y2 | u2 | δ2 | v2 | x3 | y3 | u3 | δ3 | v3 |
| 0.088931 | 0.098075 | 0.031722 | 0.092085 | -0.00377 | 0.126225 | 0.098075 | 0.034195 | 0.093568 | -0.00442 | 0.16065 | 0.098075 | 0.035059 | 0.088038 | -0.00657 |
| 0.088931 | 0.095207 | 0.034841 | 0.091232 | -0.00596 | 0.126225 | 0.095207 | 0.036766 | 0.152809 | -0.00708 | 0.16065 | 0.095207 | 0.035967 | 0.103533 | -0.00548 |
| 0.088931 | 0.092338 | 0.037291 | 0.098104 | -0.0058 | 0.126225 | 0.092338 | 0.036693 | 0.095122 | -0.00598 | 0.16065 | 0.092338 | 0.035185 | 0.094736 | -0.00495 |
| 0.088931 | 0.089469 | 0.036821 | 0.032771 | -0.00573 | 0.126225 | 0.089469 | 0.035104 | 0.043251 | -0.0047 | 0.16065 | 0.089469 | 0.031537 | 0.064851 | -0.00334 |
| 0.088931 | 0.0866 | 0.036892 | 0.078351 | -0.00578 | 0.126225 | 0.0866 | 0.035299 | 0.071835 | -0.00466 | 0.16065 | 0.0866 | 0.032317 | 0.079758 | -0.00319 |
| 0.088931 | 0.083732 | 0.037359 | 0.07782 | -0.0064 | 0.126225 | 0.083732 | 0.035869 | 0.073015 | -0.00549 | 0.16065 | 0.083732 | 0.034798 | 0.074602 | -0.00413 |
| 0.088931 | 0.080863 | 0.037784 | 0.064704 | -0.00666 | 0.126225 | 0.080863 | 0.036503 | -0.02734 | -0.0056 | 0.16065 | 0.080863 | 0.035878 | 0.063938 | -0.00463 |
| 0.088931 | 0.077994 | 0.037864 | 0.083086 | -0.00596 | 0.126225 | 0.077994 | 0.036548 | 0.088796 | -0.00458 | 0.16065 | 0.077994 | 0.036278 | 0.087571 | -0.00385 |
| 0.088931 | 0.075125 | 0.037655 | 0.086707 | -0.00519 | 0.126225 | 0.075125 | 0.036101 | -0.04339 | -0.00384 | 0.16065 | 0.075125 | 0.035692 | 0.091688 | -0.0034 |
| 0.088931 | 0.072257 | 0.037512 | 0.060558 | -0.00497 | 0.126225 | 0.072257 | 0.036152 | 0.062513 | -0.00388 | 0.16065 | 0.072257 | 0.035251 | 0.064691 | -0.0035 |
| 0.088931 | 0.069388 | 0.037689 | 0.055164 | -0.00482 | 0.126225 | 0.069388 | 0.036765 | 0.060323 | -0.00413 | 0.16065 | 0.069388 | 0.036382 | 0.061579 | -0.00386 |
| 0.088931 | 0.066519 | 0.037799 | 0.074557 | -0.00438 | 0.126225 | 0.066519 | 0.03723 | 0.090117 | -0.00369 | 0.16065 | 0.066519 | 0.037063 | 0.076402 | -0.00336 |
| 0.088931 | 0.06365 | 0.037644 | 0.076104 | -0.00347 | 0.126225 | 0.06365 | 0.037108 | 0.071708 | -0.00291 | 0.16065 | 0.06365 | 0.036723 | 0.075049 | -0.00232 |
| 0.088931 | 0.060782 | 0.037508 | 0.019529 | -0.00255 | 0.126225 | 0.060782 | 0.036707 | -0.02753 | -0.00227 | 0.16065 | 0.060782 | 0.036342 | 0.032945 | -0.0017 |
| 0.088931 | 0.057913 | 0.037558 | 0.046315 | -0.00176 | 0.126225 | 0.057913 | 0.036757 | 0.047265 | -0.00169 | 0.16065 | 0.057913 | 0.036537 | 0.042948 | -0.0012 |
| 0.088931 | 0.055044 | 0.037726 | 0.153637 | -0.00081 | 0.126225 | 0.055044 | 0.037155 | 0.036971 | -0.00088 | 0.16065 | 0.055044 | 0.036863 | 0.092657 | -0.00038 |
| 0.088931 | 0.052175 | 0.037711 | 0.056929 | 0.000316 | 0.126225 | 0.052175 | 0.037327 | 0.054724 | 0.000245 | 0.16065 | 0.052175 | 0.036758 | 0.054142 | 0.000754 |
| 0.088931 | 0.049307 | 0.037394 | 0.055134 | 0.001215 | 0.126225 | 0.049307 | 0.036304 | 0.055237 | 0.000928 | 0.16065 | 0.049307 | 0.034604 | 0.051857 | 0.001039 |
| 0.088931 | 0.046438 | 0.03698 | 0.020757 | 0.001888 | 0.126225 | 0.046438 | 0.03537 | 0.030987 | 0.001441 | 0.16065 | 0.046438 | 0.030518 | 0.010232 | 0.001008 |
| 0.088931 | 0.043569 | 0.037121 | 0.004838 | 0.002803 | 0.126225 | 0.043569 | 0.035902 | 0.014726 | 0.002238 | 0.16065 | 0.043569 | 0.03113 | 0.03398 | 0.001379 |
| 0.088931 | 0.0407 | 0.037203 | 0.046822 | 0.003367 | 0.126225 | 0.0407 | 0.036134 | 0.046863 | 0.002829 | 0.16065 | 0.0407 | 0.033255 | 0.062652 | 0.001784 |
| 0.088931 | 0.037832 | 0.03672 | 0.046337 | 0.003172 | 0.126225 | 0.037832 | 0.035156 | 0.050412 | 0.002663 | 0.16065 | 0.037832 | 0.032604 | 0.058391 | 0.00176 |
| 0.088931 | 0.034963 | 0.036208 | -0.00784 | 0.002767 | 0.126225 | 0.034963 | 0.034454 | 0.016004 | 0.00234 | 0.16065 | 0.034963 | 0.031819 | -0.02613 | 0.001536 |
| 0.088931 | 0.032094 | 0.036344 | 0.02093 | 0.002925 | 0.126225 | 0.032094 | 0.035026 | 0.017407 | 0.002543 | 0.16065 | 0.032094 | 0.03212 | 0.020834 | 0.001568 |
| 0.088931 | 0.029225 | 0.03683 | 0.037941 | 0.00316 | 0.126225 | 0.029225 | 0.035653 | 0.037009 | 0.002584 | 0.16065 | 0.029225 | 0.033678 | 0.040948 | 0.00181 |
| 0.088931 | 0.026357 | 0.036368 | 0.030768 | 0.002629 | 0.126225 | 0.026357 | 0.034701 | 0.030219 | 0.001982 | 0.16065 | 0.026357 | 0.032563 | 0.032911 | 0.001383 |
| 0.088931 | 0.023488 | 0.035153 | 0.028475 | 0.001734 | 0.126225 | 0.023488 | 0.032076 | 0.037352 | 0.001218 | 0.16065 | 0.023488 | 0.03008 | 0.04604 | 0.000618 |
| 0.088931 | 0.020619 | 0.03338 | 0.026711 | 0.001168 | 0.126225 | 0.020619 | 0.030801 | 0.070056 | 0.000737 | 0.16065 | 0.020619 | 0.029043 | -0.13623 | 0.000274 |
| 0.088931 | 0.01775 | 0.031094 | 0.024771 | 0.000959 | 0.126225 | 0.01775 | 0.03037 | 0.028073 | 0.000404 | 0.16065 | 0.01775 | 0.029211 | 0.043923 | 3.35E-06 |
| 0.088931 | 0.014882 | 0.028176 | 0.018977 | 0.000652 | 0.126225 | 0.014882 | 0.028184 | 0.020898 | 6.8E-05 | 0.16065 | 0.014882 | 0.028222 | 0.024981 | -0.00019 |
| 0.088931 | 0.012013 | 0.021129 | 0.020031 | 0.00024 | 0.126225 | 0.012013 | 0.023391 | 0.021576 | -0.00044 | 0.16065 | 0.012013 | 0.025378 | 0.025893 | -0.00034 |
| 0.088931 | 0.009144 | 0.015009 | 0.028518 | 1.79E-05 | 0.126225 | 0.009144 | 0.018939 | 0.03845 | -0.00051 | 0.16065 | 0.009144 | 0.02272 | 0.044885 | -0.0005 |
| 0.088931 | 0.006275 | 0.01157 | 0.032306 | -1.8E-05 | 0.126225 | 0.006275 | 0.01705 | 0.020094 | -0.00047 | 0.16065 | 0.006275 | 0.021475 | 0.026076 | -0.00057 |
| 0.088931 | 0.003407 | 0.008631 | 0.015091 | -8E-05 | 0.126225 | 0.003407 | 0.012652 | 0.010295 | -0.00042 | 0.16065 | 0.003407 | 0.019047 | 0.006839 | -0.00049 |

Raw Data of 3 x-locations for 5Hz With Trip.

| | | U∞ | 0.079 | m/s | | Spec U∞ | 0.0857 | 0.0808 | m/s | | | | | |
|---|---|---|---|---|---|---|---|---|---|---|---|---|---|---|
| es 1:499, conversion factor xy (px -> m): 0.00017898, conversion factor uv (px/frame -> m/s): 0.026833 | | | | | | | | | | | | | | |
| 99% U∞ | 0.078126 | m/s | 0.066401 | δ (m) | 99% U∞ | 0.078126 | m/s | 0.052083 | δ (m) | 99% U∞ | 0.078126 | m/s | 0.054946 | δ (m) |
| x1 | y1 | u1 | δ1 | v1 | x2 | y2 | u2 | δ2 | v2 | x3 | y3 | u3 | δ3 | v3 |
| 0.088773 | 0.097901 | 0.068636 | 0.093002 | -0.00438 | 0.126001 | 0.097901 | 0.068199 | 0.091673 | -0.00702 | 0.160365 | 0.097901 | 0.066502 | 0.088383 | -0.00855 |
| 0.088773 | 0.095038 | 0.074183 | 0.080008 | -0.00927 | 0.126001 | 0.095038 | 0.072763 | 0.127553 | -0.01079 | 0.160365 | 0.095038 | 0.069999 | 0.028499 | -0.01192 |
| 0.088773 | 0.092174 | 0.074934 | 0.098781 | -0.01027 | 0.126001 | 0.092174 | 0.07229 | 0.110129 | -0.00999 | 0.160365 | 0.092174 | 0.070349 | 0.109296 | -0.00809 |
| 0.088773 | 0.08931 | 0.073551 | 0.067917 | -0.00873 | 0.126001 | 0.08931 | 0.07136 | 0.13571 | -0.00818 | 0.160365 | 0.08931 | 0.069048 | -0.07132 | -0.00576 |
| 0.088773 | 0.086447 | 0.074163 | 0.077706 | -0.00844 | 0.126001 | 0.086447 | 0.070942 | 0.069858 | -0.00771 | 0.160365 | 0.086447 | 0.06921 | 0.07408 | -0.00611 |
| 0.088773 | 0.083583 | 0.075462 | 0.076731 | -0.00926 | 0.126001 | 0.083583 | 0.072182 | 0.073281 | -0.00814 | 0.160365 | 0.083583 | 0.071274 | 0.071943 | -0.00696 |
| 0.088773 | 0.080719 | 0.076575 | 0.071005 | -0.00951 | 0.126001 | 0.080719 | 0.073834 | 0.053705 | -0.00818 | 0.160365 | 0.080719 | 0.07296 | 0.026481 | -0.00742 |
| 0.088773 | 0.077856 | 0.077032 | 0.040784 | -0.00851 | 0.126001 | 0.077856 | 0.074289 | 0.099339 | -0.00704 | 0.160365 | 0.077856 | 0.073233 | 0.086138 | -0.00639 |
| 0.088773 | 0.074992 | 0.077117 | 0.047747 | -0.00753 | 0.126001 | 0.074992 | 0.073778 | 0.020848 | -0.00655 | 0.160365 | 0.074992 | 0.071541 | 0.025483 | -0.00606 |
| 0.088773 | 0.072128 | 0.077223 | 0.066993 | -0.00747 | 0.126001 | 0.072128 | 0.074008 | 0.053133 | -0.00699 | 0.160365 | 0.072128 | 0.071922 | 0.046401 | -0.00667 |
| 0.088773 | 0.069265 | 0.077726 | 0.061165 | -0.0078 | 0.126001 | 0.069265 | 0.074629 | 0.042029 | -0.00771 | 0.160365 | 0.069265 | 0.072612 | 0.055174 | -0.00733 |
| 0.088773 | 0.066401 | 0.077868 | 0.068074 | -0.00783 | 0.126001 | 0.066401 | 0.074996 | 0.089762 | -0.00746 | 0.160365 | 0.066401 | 0.073733 | 0.129649 | -0.00696 |
| 0.088773 | 0.063537 | 0.077426 | 0.067769 | -0.00704 | 0.126001 | 0.063537 | 0.074613 | 0.086621 | -0.00671 | 0.160365 | 0.063537 | 0.073534 | 0.115154 | -0.00596 |
| 0.088773 | 0.060674 | 0.076952 | 0.074404 | -0.00634 | 0.126001 | 0.060674 | 0.074177 | -0.0479 | -0.00623 | 0.160365 | 0.060674 | 0.073279 | 0.037886 | -0.0055 |
| 0.088773 | 0.05781 | 0.076707 | 0.082383 | -0.00582 | 0.126001 | 0.05781 | 0.074281 | 0.041322 | -0.00623 | 0.160365 | 0.05781 | 0.073888 | 0.026723 | -0.00599 |
| 0.088773 | 0.054946 | 0.076542 | 0.06856 | -0.0053 | 0.126001 | 0.054946 | 0.074949 | 0.000641 | -0.00644 | 0.160365 | 0.054946 | 0.074278 | 0.087402 | -0.0063 |
| 0.088773 | 0.052083 | 0.076208 | 0.060306 | -0.00447 | 0.126001 | 0.052083 | 0.075116 | 0.057627 | -0.00581 | 0.160365 | 0.052083 | 0.073939 | 0.05528 | -0.00547 |
| 0.088773 | 0.049219 | 0.075541 | 0.058495 | -0.0033 | 0.126001 | 0.049219 | 0.073562 | 0.058836 | -0.00455 | 0.160365 | 0.049219 | 0.070189 | 0.052382 | -0.00368 |
| 0.088773 | 0.046355 | 0.074742 | -0.0289 | -0.00241 | 0.126001 | 0.046355 | 0.072203 | 0.015783 | -0.00357 | 0.160365 | 0.046355 | 0.063003 | 0.035466 | -0.00281 |
| 0.088773 | 0.043492 | 0.074871 | 0.015955 | -0.00185 | 0.126001 | 0.043492 | 0.072758 | -0.01062 | -0.0032 | 0.160365 | 0.043492 | 0.06698 | 0.029575 | -0.00297 |
| 0.088773 | 0.040628 | 0.07521 | 0.051095 | -0.00151 | 0.126001 | 0.040628 | 0.073042 | 0.049944 | -0.00306 | 0.160365 | 0.040628 | 0.069273 | 0.05138 | -0.00297 |
| 0.088773 | 0.037764 | 0.074412 | 0.048052 | -0.00098 | 0.126001 | 0.037764 | 0.071479 | 0.05391 | -0.00241 | 0.160365 | 0.037764 | 0.066915 | 0.055403 | -0.00291 |
| 0.088773 | 0.034901 | 0.073378 | 0.14717 | -0.0003 | 0.126001 | 0.034901 | 0.0703 | -0.01099 | -0.00167 | 0.160365 | 0.034901 | 0.065095 | 0.008593 | -0.00239 |
| 0.088773 | 0.032037 | 0.073257 | 0.001668 | 0.000212 | 0.126001 | 0.032037 | 0.070788 | 0.005049 | -0.0014 | 0.160365 | 0.032037 | 0.066514 | 0.002071 | -0.00228 |
| 0.088773 | 0.029173 | 0.073716 | 0.055229 | 0.000509 | 0.126001 | 0.029173 | 0.071567 | 0.045449 | -0.00157 | 0.160365 | 0.029173 | 0.067623 | 0.039641 | -0.00248 |
| 0.088773 | 0.02631 | 0.073231 | 0.03584 | 0.000407 | 0.126001 | 0.02631 | 0.070413 | 0.034279 | -0.00132 | 0.160365 | 0.02631 | 0.06475 | 0.032873 | -0.00232 |
| 0.088773 | 0.023446 | 0.071761 | 0.029771 | 0.000355 | 0.126001 | 0.023446 | 0.067641 | 0.033332 | -0.00071 | 0.160365 | 0.023446 | 0.058914 | 0.049361 | -0.00158 |
| 0.088773 | 0.020583 | 0.068879 | 0.025836 | 0.000798 | 0.126001 | 0.020583 | 0.064604 | 0.060893 | 0.000304 | 0.160365 | 0.020583 | 0.056791 | -0.11855 | -0.0008 |
| 0.088773 | 0.017719 | 0.063838 | 0.022307 | 0.001445 | 0.126001 | 0.017719 | 0.063644 | 0.042161 | 0.000574 | 0.160365 | 0.017719 | 0.05723 | -7.31347 | -0.00158 |
| 0.088773 | 0.014855 | 0.054921 | 0.020496 | 0.001203 | 0.126001 | 0.014855 | 0.061947 | 0.023675 | 0.000652 | 0.160365 | 0.014855 | 0.057239 | 0.033503 | -0.00232 |
| 0.088773 | 0.011992 | 0.043141 | 0.018743 | 3.88E-05 | 0.126001 | 0.011992 | 0.056694 | 0.020717 | 0.000261 | 0.160365 | 0.011992 | 0.054031 | 0.025173 | -0.00173 |
| 0.088773 | 0.009128 | 0.028301 | 0.039382 | -0.00036 | 0.126001 | 0.009128 | 0.04966 | 0.03896 | -0.00041 | 0.160365 | 0.009128 | 0.048796 | 0.038436 | -0.00115 |
| 0.088773 | 0.006264 | 0.023585 | -0.07671 | -0.00074 | 0.126001 | 0.006264 | 0.046928 | 0.017952 | -0.00071 | 0.160365 | 0.006264 | 0.045931 | 0.019616 | -0.00089 |
| 0.088773 | 0.003401 | 0.025467 | 0.010432 | -0.00168 | 0.126001 | 0.003401 | 0.039284 | 0.006763 | -0.00093 | 0.160365 | 0.003401 | 0.039026 | 0.006808 | -0.00034 |

Raw Data of 3 x-locations for 10Hz With Trip.

| | | U∞ | 0.158 | m/s | | Spec U∞ | 0.1686 | 0.1585 | m/s | | | | | |
|---|---|---|---|---|---|---|---|---|---|---|---|---|---|---|
| es 1:499, conversion factor xy (px -> m): 0.00018475, conversion factor uv (px/frame -> m/s): 0.055481 | | | | | | | | | | | | | | |
| 99% U∞ | 0.156784 | m/s | 0.085285 | δ (m) | 99% U∞ | 0.156784 | m/s | 0.053763 | δ (m) | 99% U∞ | 0.156784 | m/s | 0.056719 | δ (m) |
| x1 | y1 | u1 | δ1 | v1 | x2 | y2 | u2 | δ2 | v2 | x3 | y3 | u3 | δ3 | v3 |
| 0.091638 | 0.10106 | 0.133828 | 0.09694 | -0.0032 | 0.130066 | 0.10106 | 0.141977 | 0.095767 | -0.00806 | 0.165539 | 0.10106 | 0.150604 | 0.084875 | -0.01058 |
| 0.091638 | 0.098104 | 0.150296 | 0.094603 | -0.00695 | 0.130066 | 0.098104 | 0.150246 | 0.080112 | -0.01184 | 0.165539 | 0.098104 | 0.151732 | 14.39789 | -0.0143 |
| 0.091638 | 0.095148 | 0.155773 | 0.096569 | -0.00576 | 0.130066 | 0.095148 | 0.15132 | 0.101057 | -0.01006 | 0.165539 | 0.095148 | 0.151731 | 0.098637 | -0.01197 |
| 0.091638 | 0.092192 | 0.153671 | 0.10595 | -0.0054 | 0.130066 | 0.092192 | 0.148587 | 0.10289 | -0.00825 | 0.165539 | 0.092192 | 0.14745 | 0.102996 | -0.00936 |
| 0.091638 | 0.089236 | 0.153002 | 0.08587 | -0.00529 | 0.130066 | 0.089236 | 0.146323 | 0.080031 | -0.00786 | 0.165539 | 0.089236 | 0.144897 | 0.080679 | -0.00994 |
| 0.091638 | 0.08628 | 0.156324 | 0.085285 | -0.00548 | 0.130066 | 0.08628 | 0.149682 | 0.074995 | -0.00963 | 0.165539 | 0.08628 | 0.149003 | 0.07715 | -0.01164 |
| 0.091638 | 0.083324 | 0.157691 | 0.07589 | -0.00551 | 0.130066 | 0.083324 | 0.151542 | 0.145591 | -0.0098 | 0.165539 | 0.083324 | 0.151522 | 0.114227 | -0.01203 |
| 0.091638 | 0.080368 | 0.15733 | 0.079232 | -0.00429 | 0.130066 | 0.080368 | 0.151294 | 0.089215 | -0.00794 | 0.165539 | 0.080368 | 0.151019 | 0.085991 | -0.00977 |
| 0.091638 | 0.077412 | 0.155908 | 0.079824 | -0.00284 | 0.130066 | 0.077412 | 0.149459 | 0.126965 | -0.00715 | 0.165539 | 0.077412 | 0.147988 | 0.091287 | -0.00908 |
| 0.091638 | 0.074456 | 0.154835 | 0.065118 | -0.00177 | 0.130066 | 0.074456 | 0.149022 | 0.061036 | -0.00728 | 0.165539 | 0.074456 | 0.146115 | 0.062229 | -0.01008 |
| 0.091638 | 0.0715 | 0.155452 | 0.054245 | -0.00161 | 0.130066 | 0.0715 | 0.150732 | 0.061686 | -0.00788 | 0.165539 | 0.0715 | 0.148694 | 0.063962 | -0.01034 |
| 0.091638 | 0.068544 | 0.15568 | 0.083176 | -0.00206 | 0.130066 | 0.068544 | 0.152555 | -0.0305 | -0.00717 | 0.165539 | 0.068544 | 0.151867 | 0.755736 | -0.00859 |
| 0.091638 | 0.065587 | 0.155457 | 0.074138 | -0.00161 | 0.130066 | 0.065587 | 0.152681 | 0.077223 | -0.00596 | 0.165539 | 0.065587 | 0.151846 | 0.087442 | -0.00601 |
| 0.091638 | 0.062631 | 0.154998 | 0.00499 | -0.00119 | 0.130066 | 0.062631 | 0.151639 | 0.021037 | -0.00518 | 0.165539 | 0.062631 | 0.151178 | 0.050781 | -0.00534 |
| 0.091638 | 0.059675 | 0.15509 | 0.054958 | -0.00116 | 0.130066 | 0.059675 | 0.152005 | 0.052535 | -0.00486 | 0.165539 | 0.059675 | 0.152576 | 0.053837 | -0.00535 |
| 0.091638 | 0.056719 | 0.156151 | 0.053958 | -0.00088 | 0.130066 | 0.056719 | 0.153983 | 0.051936 | -0.00474 | 0.165539 | 0.056719 | 0.154706 | 0.061857 | -0.00502 |
| 0.091638 | 0.053763 | 0.156828 | 0.05361 | -0.00031 | 0.130066 | 0.053763 | 0.155714 | 0.054585 | -0.00368 | 0.165539 | 0.053763 | 0.153511 | 0.054666 | -0.00361 |
| 0.091638 | 0.050807 | 0.155967 | 0.052675 | 0.000424 | 0.130066 | 0.050807 | 0.151865 | 0.055152 | -0.00237 | 0.165539 | 0.050807 | 0.14279 | 0.053108 | -0.0022 |
| 0.091638 | 0.047851 | 0.154675 | 0.038476 | 0.001023 | 0.130066 | 0.047851 | 0.148518 | 0.037805 | -0.00145 | 0.165539 | 0.047851 | 0.124812 | 0.038653 | -0.00145 |
| 0.091638 | 0.044895 | 0.15534 | 0.034842 | 0.001584 | 0.130066 | 0.044895 | 0.15095 | 0.02374 | -0.00089 | 0.165539 | 0.044895 | 0.135087 | 0.035351 | -0.00164 |
| 0.091638 | 0.041939 | 0.155765 | 0.043405 | 0.001432 | 0.130066 | 0.041939 | 0.151765 | 0.047687 | -0.00118 | 0.165539 | 0.041939 | 0.141807 | 0.049344 | -0.00222 |
| 0.091638 | 0.038983 | 0.15371 | 0.043146 | 0.000964 | 0.130066 | 0.038983 | 0.149184 | 0.050899 | -0.00153 | 0.165539 | 0.038983 | 0.135827 | 0.102281 | -0.00237 |
| 0.091638 | 0.036027 | 0.151527 | 0.058471 | 0.001024 | 0.130066 | 0.036027 | 0.147299 | -0.0305 | -0.00133 | 0.165539 | 0.036027 | 0.134849 | 0.009393 | -0.00187 |
| 0.091638 | 0.033071 | 0.150834 | 0.01808 | 0.001188 | 0.130066 | 0.033071 | 0.147721 | -0.01514 | -0.00111 | 0.165539 | 0.033071 | 0.137283 | 0.008382 | -0.00124 |
| 0.091638 | 0.030115 | 0.152008 | 0.037789 | 0.001225 | 0.130066 | 0.030115 | 0.148276 | 0.034173 | -0.0014 | 0.165539 | 0.030115 | 0.139618 | 0.039848 | -0.00071 |
| 0.091638 | 0.027159 | 0.150168 | 0.031034 | 0.000559 | 0.130066 | 0.027159 | 0.142079 | 0.031445 | -0.00203 | 0.165539 | 0.027159 | 0.134405 | 0.034545 | -0.00093 |
| 0.091638 | 0.024203 | 0.145121 | 0.028617 | 0.000727 | 0.130066 | 0.024203 | 0.131938 | 0.033722 | -0.00175 | 0.165539 | 0.024203 | 0.125449 | 0.048164 | -0.00086 |
| 0.091638 | 0.021247 | 0.13731 | 0.029366 | 0.000851 | 0.130066 | 0.021247 | 0.124223 | 0.049539 | -0.00202 | 0.165539 | 0.021247 | 0.121583 | 0.263014 | -0.00037 |
| 0.091638 | 0.018291 | 0.130219 | 0.025779 | 0.00055 | 0.130066 | 0.018291 | 0.120821 | 0.031587 | -0.00285 | 0.165539 | 0.018291 | 0.121153 | 0.033064 | -3.9E-05 |
| 0.091638 | 0.015335 | 0.119734 | 0.020979 | 0.000199 | 0.130066 | 0.015335 | 0.112826 | 0.025219 | -0.00319 | 0.165539 | 0.015335 | 0.114023 | 0.026595 | 8.27E-07 |
| 0.091638 | 0.012378 | 0.100332 | 0.018048 | 0.000601 | 0.130066 | 0.012378 | 0.099681 | 0.02399 | -0.00408 | 0.165539 | 0.012378 | 0.102798 | 0.028105 | 0.000318 |
| 0.091638 | 0.009422 | 0.070899 | 0.024054 | 0.000913 | 0.130066 | 0.009422 | 0.085143 | 0.029085 | -0.00328 | 0.165539 | 0.009422 | 0.092651 | 0.048688 | 0.001317 |
| 0.091638 | 0.006466 | 0.053547 | 0.041115 | 0.000685 | 0.130066 | 0.006466 | 0.074373 | 0.024961 | -0.00149 | 0.165539 | 0.006466 | 0.087823 | 0.026035 | 0.002209 |
| 0.091638 | 0.00351 | 0.044739 | 0.012302 | 0.000402 | 0.130066 | 0.00351 | 0.061201 | 0.008993 | 0.000342 | 0.165539 | 0.00351 | 0.077406 | 0.00711 | 0.002461 |

Raw Data of 3 x-locations for 20Hz With Trip.

| | | U∞ | 0.230 | m/s | | Spec U∞ | 0.2501 | 0.2346 | m/s | | | | | |
|---|---|---|---|---|---|---|---|---|---|---|---|---|---|---|
| es 1:499, conversion factor xy (px -> m): 0.00017845, conversion factor uv (px/frame -> m/s): 0.07138 | | | | | | | | | | | | | | |
| 99% U∞ | 0.227291 | m/s | 0.064398 | δ (m) | 99% U∞ | 0.227291 | m/s | 0.06335 | δ (m) | 99% U∞ | 0.227291 | m/s | 0.066205 | δ (m) |
| x1 | y1 | u1 | δ1 | v1 | x2 | y2 | u2 | δ2 | v2 | x3 | y3 | u3 | δ3 | v3 |
| 0.088512 | 0.097613 | 0.198479 | 0.089666 | 0.002284 | 0.12563 | 0.097613 | 0.19958 | 0.094001 | -0.00392 | 0.159892 | 0.097613 | 0.212794 | 0.077221 | -0.00687 |
| 0.088512 | 0.094758 | 0.208831 | 0.088696 | 0.005236 | 0.12563 | 0.094758 | 0.221487 | 0.03748 | -0.00503 | 0.159892 | 0.094758 | 0.214824 | 0.169757 | -0.00739 |
| 0.088512 | 0.091902 | 0.217526 | 0.098003 | -0.00182 | 0.12563 | 0.091902 | 0.221776 | 0.093633 | -0.00572 | 0.159892 | 0.091902 | 0.214349 | 0.096751 | -0.00521 |
| 0.088512 | 0.089047 | 0.212955 | 0.10103 | -0.00175 | 0.12563 | 0.089047 | 0.21268 | 0.13205 | -0.00322 | 0.159892 | 0.089047 | 0.206728 | 0.106199 | -0.00256 |
| 0.088512 | 0.086192 | 0.209539 | 0.082153 | -0.00672 | 0.12563 | 0.086192 | 0.21171 | 0.078846 | -0.00594 | 0.159892 | 0.086192 | 0.203305 | -0.08721 | -0.0056 |
| 0.088512 | 0.083337 | 0.222088 | 0.078658 | -0.00559 | 0.12563 | 0.083337 | 0.217766 | 0.331636 | -0.00948 | 0.159892 | 0.083337 | 0.2037 | 0.067278 | -0.00795 |
| 0.088512 | 0.080482 | 0.225263 | 0.086064 | -0.00784 | 0.12563 | 0.080482 | 0.217656 | 0.090134 | -0.01026 | 0.159892 | 0.080482 | 0.207894 | -0.03419 | -0.0084 |
| 0.088512 | 0.077626 | 0.224226 | 0.080477 | -0.00734 | 0.12563 | 0.077626 | 0.214806 | 0.088548 | -0.00834 | 0.159892 | 0.077626 | 0.208377 | 0.105579 | -0.00622 |
| 0.088512 | 0.074771 | 0.221157 | 0.134878 | -0.00637 | 0.12563 | 0.074771 | 0.211542 | 0.057074 | -0.00719 | 0.159892 | 0.074771 | 0.206445 | -0.03255 | -0.00513 |
| 0.088512 | 0.071916 | 0.220865 | 0.064489 | -0.00597 | 0.12563 | 0.071916 | 0.214083 | 0.065733 | -0.00769 | 0.159892 | 0.071916 | 0.207 | 0.063969 | -0.00785 |
| 0.088512 | 0.069061 | 0.223336 | 0.064859 | -0.00652 | 0.12563 | 0.069061 | 0.220183 | 0.062659 | -0.0087 | 0.159892 | 0.069061 | 0.214291 | 0.060053 | -0.00827 |
| 0.088512 | 0.066205 | 0.226024 | 0.064398 | -0.00747 | 0.12563 | 0.066205 | 0.223353 | -0.02006 | -0.00843 | 0.159892 | 0.066205 | 0.218412 | 0.087341 | -0.00711 |
| 0.088512 | 0.06335 | 0.228025 | 0.066611 | -0.00713 | 0.12563 | 0.06335 | 0.223484 | 0.068855 | -0.00795 | 0.159892 | 0.06335 | 0.217212 | 0.08158 | -0.0062 |
| 0.088512 | 0.060495 | 0.228668 | -0.00038 | -0.0065 | 0.12563 | 0.060495 | 0.221509 | 0.081498 | -0.0081 | 0.159892 | 0.060495 | 0.215634 | 0.034011 | -0.0069 |
| 0.088512 | 0.05764 | 0.228604 | 0.041624 | -0.00677 | 0.12563 | 0.05764 | 0.220723 | 0.045485 | -0.00922 | 0.159892 | 0.05764 | 0.21689 | 0.0368 | -0.00769 |
| 0.088512 | 0.054785 | 0.228370 | 0.051162 | -0.00696 | 0.12563 | 0.054785 | 0.222266 | 0.032941 | -0.00975 | 0.159892 | 0.054785 | 0.218315 | 0.070753 | -0.00819 |
| 0.088512 | 0.051929 | 0.227519 | 0.051545 | -0.00616 | 0.12563 | 0.051929 | 0.222922 | 0.054523 | -0.00908 | 0.159892 | 0.051929 | 0.21671 | 0.05426 | -0.00746 |
| 0.088512 | 0.049074 | 0.22582 | 0.050812 | -0.00448 | 0.12563 | 0.049074 | 0.218113 | 0.053604 | -0.00713 | 0.159892 | 0.049074 | 0.203747 | 0.051869 | -0.00589 |
| 0.088512 | 0.046219 | 0.223402 | -0.00631 | -0.00275 | 0.12563 | 0.046219 | 0.212329 | 0.016199 | -0.00571 | 0.159892 | 0.046219 | 0.179696 | 0.035215 | -0.00502 |
| 0.088512 | 0.043364 | 0.223614 | 1.339433 | -0.00148 | 0.12563 | 0.043364 | 0.213752 | 0.010974 | -0.00591 | 0.159892 | 0.043364 | 0.192045 | 0.02106 | -0.00478 |
| 0.088512 | 0.040508 | 0.223606 | 0.0439 | -0.00137 | 0.12563 | 0.040508 | 0.214945 | 0.051308 | -0.0061 | 0.159892 | 0.040508 | 0.196557 | 0.047258 | -0.00508 |
| 0.088512 | 0.037653 | 0.220503 | 0.043612 | -0.00083 | 0.12563 | 0.037653 | 0.211682 | 0.052588 | -0.00533 | 0.159892 | 0.037653 | 0.183555 | 0.068811 | -0.00539 |
| 0.088512 | 0.034798 | 0.217251 | -0.02253 | 0.000269 | 0.12563 | 0.034798 | 0.208697 | 0.020535 | -0.00424 | 0.159892 | 0.034798 | 0.179548 | 0.026602 | -0.00365 |
| 0.088512 | 0.031943 | 0.217751 | 0.018085 | 0.00138 | 0.12563 | 0.031943 | 0.212419 | 0.019518 | -0.00393 | 0.159892 | 0.031943 | 0.19618 | 0.024204 | -0.00395 |
| 0.088512 | 0.029088 | 0.219717 | 0.032448 | 0.002198 | 0.12563 | 0.029088 | 0.215837 | 0.034615 | -0.00423 | 0.159892 | 0.029088 | 0.207659 | 0.042537 | -0.0039 |
| 0.088512 | 0.026232 | 0.213281 | 0.029736 | 0.002072 | 0.12563 | 0.026232 | 0.209921 | 0.030735 | -0.00426 | 0.159892 | 0.026232 | 0.203491 | 0.029826 | -0.00288 |
| 0.088512 | 0.023377 | 0.201866 | 0.030819 | 0.001419 | 0.12563 | 0.023377 | 0.198906 | 0.03874 | -0.00301 | 0.159892 | 0.023377 | 0.184582 | 0.038637 | -0.00218 |
| 0.088512 | 0.020522 | 0.192111 | -0.04189 | 0.002576 | 0.12563 | 0.020522 | 0.193631 | 0.052921 | -0.00216 | 0.159892 | 0.020522 | 0.176591 | -0.06125 | -0.00106 |
| 0.088512 | 0.017667 | 0.19372 | 0.028632 | 0.003178 | 0.12563 | 0.017667 | 0.190665 | 0.029801 | -0.00174 | 0.159892 | 0.017667 | 0.178361 | 0.03036 | -0.00046 |
| 0.088512 | 0.014811 | 0.184979 | 0.017874 | 0.003331 | 0.12563 | 0.014811 | 0.182047 | 0.020854 | -0.00092 | 0.159892 | 0.014811 | 0.167355 | 0.022091 | 0.000469 |
| 0.088512 | 0.011956 | 0.145529 | 0.017866 | 0.002546 | 0.12563 | 0.011956 | 0.160667 | 0.017845 | -0.00015 | 0.159892 | 0.011956 | 0.143849 | 0.021881 | 0.002093 |
| 0.088512 | 0.009101 | 0.106023 | 0.025656 | 0.001479 | 0.12563 | 0.009101 | 0.128362 | 0.020714 | -0.001 | 0.159892 | 0.009101 | 0.119845 | 0.029919 | 0.001245 |
| 0.088512 | 0.006246 | 0.085109 | 0.03374 | 0.00254 | 0.12563 | 0.006246 | 0.10404 | 0.018526 | -0.00074 | 0.159892 | 0.006246 | 0.105109 | 0.019956 | -0.00054 |
| 0.088512 | 0.003391 | 0.070343 | 0.010955 | 0.001345 | 0.12563 | 0.003391 | 0.075385 | 0.010223 | -0.00105 | 0.159892 | 0.003391 | 0.079663 | 0.009674 | -0.00359 |

Raw Data of 3 x-locations for 30Hz With Trip.

| | | U∞ | 0.342 | m/s | | Spec U∞ | 0.3304 | 0.3095 | m/s | | | | | |
|---|---|---|---|---|---|---|---|---|---|---|---|---|---|---|
| es 1:499, conversion factor xy (px -> m): 0.0001793, conversion factor uv (px/frame -> m/s): 0.089648 | | | | | | | | | | | | | | |
| 99% U∞ | 0.338534 | m/s | 0.080863 | δ (m) | 99% U∞ | 0.338534 | m/s | 0.066519 | δ (m) | 99% U∞ | 0.338534 | m/s | 0.066519 | δ (m) |
| x1 | y1 | u1 | δ1 | v1 | x2 | y2 | u2 | δ2 | v2 | x3 | y3 | u3 | δ3 | v3 |
| 0.088931 | 0.098075 | 0.295418 | 0.105356 | -0.00108 | 0.126225 | 0.098075 | 0.243011 | 0.091352 | -0.00427 | 0.16065 | 0.098075 | 0.233581 | 0.089787 | -0.00135 |
| 0.088931 | 0.095207 | 0.278428 | -0.01066 | -0.00024 | 0.126225 | 0.095207 | 0.283767 | 0.07133 | -0.00819 | 0.16065 | 0.095207 | 0.269906 | 0.031907 | 0.003581 |
| 0.088931 | 0.092338 | 0.280057 | 0.105366 | -0.004 | 0.126225 | 0.092338 | 0.290347 | 0.109005 | -0.00159 | 0.16065 | 0.092338 | 0.273016 | 0.13818 | 0.001713 |
| 0.088931 | 0.089469 | 0.267181 | 0.078429 | -0.008 | 0.126225 | 0.089469 | 0.282053 | 0.132631 | -1.8E-05 | 0.16065 | 0.089469 | 0.268916 | 0.025305 | 0.004466 |
| 0.088931 | 0.0866 | 0.285722 | 0.078426 | -0.00205 | 0.126225 | 0.0866 | 0.278299 | 0.074667 | -0.00043 | 0.16065 | 0.0866 | 0.272028 | 0.065603 | -0.00113 |
| 0.088931 | 0.083732 | 0.304256 | 0.055673 | -0.00253 | 0.126225 | 0.083732 | 0.292779 | 0.059222 | -0.00117 | 0.16065 | 0.083732 | 0.281114 | 0.055511 | -0.002 |
| 0.088931 | 0.080863 | 0.30776 | 0.158225 | -0.00271 | 0.126225 | 0.080863 | 0.298134 | 0.132247 | -0.00135 | 0.16065 | 0.080863 | 0.286951 | 0.106877 | -0.00469 |
| 0.088931 | 0.077994 | 0.306619 | 0.12502 | -0.00229 | 0.126225 | 0.077994 | 0.295879 | 0.133074 | -0.00146 | 0.16065 | 0.077994 | 0.281263 | 0.125403 | -0.00565 |
| 0.088931 | 0.075125 | 0.304672 | -13.1458 | -0.0013 | 0.126225 | 0.075125 | 0.293657 | -0.03394 | -0.00124 | 0.16065 | 0.075125 | 0.277797 | -0.02029 | -0.00314 |
| 0.088931 | 0.072257 | 0.30468 | 0.030721 | -0.00244 | 0.126225 | 0.072257 | 0.294838 | 0.041877 | -0.00225 | 0.16065 | 0.072257 | 0.279624 | 0.047559 | -0.00674 |
| 0.088931 | 0.069388 | 0.307018 | 0.270943 | -0.00379 | 0.126225 | 0.069388 | 0.298964 | -0.01809 | -0.0048 | 0.16065 | 0.069388 | 0.286466 | 0.034122 | -0.00793 |
| 0.088931 | 0.066519 | 0.306569 | 0.136362 | -0.00569 | 0.126225 | 0.066519 | 0.300262 | 0.113635 | -0.00693 | 0.16065 | 0.066519 | 0.290702 | 0.092223 | -0.00726 |
| 0.088931 | 0.06365 | 0.305256 | 0.105422 | -0.00606 | 0.126225 | 0.06365 | 0.297931 | 0.091273 | -0.00777 | 0.16065 | 0.06365 | 0.285363 | 0.116549 | -0.0069 |
| 0.088931 | 0.060782 | 0.302971 | 0.174456 | -0.0066 | 0.126225 | 0.060782 | 0.293715 | 1.073078 | -0.00844 | 0.16065 | 0.060782 | 0.28248 | -0.03879 | -0.00813 |
| 0.088931 | 0.057913 | 0.302073 | -0.08881 | -0.00796 | 0.126225 | 0.057913 | 0.293588 | 0.017817 | -0.00975 | 0.16065 | 0.057913 | 0.284095 | 0.018916 | -0.01025 |
| 0.088931 | 0.055044 | 0.302786 | -1.08217 | -0.00943 | 0.126225 | 0.055044 | 0.296803 | -0.05664 | -0.01189 | 0.16065 | 0.055044 | 0.288099 | 0.221096 | -0.01136 |
| 0.088931 | 0.052175 | 0.302876 | 0.107479 | -0.01036 | 0.126225 | 0.052175 | 0.297875 | 0.068464 | -0.01199 | 0.16065 | 0.052175 | 0.287228 | 0.059673 | -0.0098 |
| 0.088931 | 0.049307 | 0.301027 | 0.086215 | -0.00935 | 0.126225 | 0.049307 | 0.290714 | 0.064712 | -0.00961 | 0.16065 | 0.049307 | 0.267597 | 0.052089 | -0.00697 |
| 0.088931 | 0.046438 | 0.298111 | -0.07515 | -0.00774 | 0.126225 | 0.046438 | 0.28181 | 0.019487 | -0.00797 | 0.16065 | 0.046438 | 0.194466 | 0.03165 | -0.00375 |
| 0.088931 | 0.043569 | 0.299065 | -0.02247 | -0.00675 | 0.126225 | 0.043569 | 0.287848 | -0.01248 | -0.00852 | 0.16065 | 0.043569 | 0.222413 | 0.035497 | -0.00621 |
| 0.088931 | 0.0407 | 0.30078 | 0.067405 | -0.00709 | 0.126225 | 0.0407 | 0.290442 | 0.057159 | -0.00947 | 0.16065 | 0.0407 | 0.263682 | 0.048489 | -0.00817 |
| 0.088931 | 0.037832 | 0.296724 | 0.065876 | -0.00673 | 0.126225 | 0.037832 | 0.282059 | 0.057412 | -0.00852 | 0.16065 | 0.037832 | 0.236111 | 0.102982 | -0.0024 |
| 0.088931 | 0.034963 | 0.292447 | 0.197272 | -0.0047 | 0.126225 | 0.034963 | 0.273785 | -2.3E-05 | -0.006 | 0.16065 | 0.034963 | 0.231601 | 0.021611 | -0.00458 |
| 0.088931 | 0.032094 | 0.291632 | 0.254867 | -0.00313 | 0.126225 | 0.032094 | 0.279094 | -0.1848 | -0.00524 | 0.16065 | 0.032094 | 0.254577 | -0.00916 | -0.00658 |
| 0.088931 | 0.029225 | 0.291029 | 0.040647 | -0.00294 | 0.126225 | 0.029225 | 0.27988 | 0.037946 | -0.00652 | 0.16065 | 0.029225 | 0.260414 | 0.047646 | -0.00874 |
| 0.088931 | 0.026357 | 0.279096 | 0.035335 | -0.00311 | 0.126225 | 0.026357 | 0.260584 | 0.034189 | -0.00873 | 0.16065 | 0.026357 | 0.248248 | 0.033712 | -0.00855 |
| 0.088931 | 0.023488 | 0.260105 | 0.031347 | -0.00294 | 0.126225 | 0.023488 | 0.232032 | 0.039155 | -0.00819 | 0.16065 | 0.023488 | 0.213034 | 0.044233 | -0.00906 |
| 0.088931 | 0.020619 | 0.231475 | 0.042906 | 0.00112 | 0.126225 | 0.020619 | 0.212531 | 0.04577 | -0.00802 | 0.16065 | 0.020619 | 0.195679 | 0.099564 | -0.00739 |
| 0.088931 | 0.01775 | 0.217695 | 0.036899 | 0.00166 | 0.126225 | 0.01775 | 0.198159 | 0.033988 | -0.00927 | 0.16065 | 0.01775 | 0.190488 | 0.039703 | -0.00576 |
| 0.088931 | 0.014882 | 0.199591 | 0.023644 | 0.002003 | 0.126225 | 0.014882 | 0.173358 | 0.027355 | -0.01128 | 0.16065 | 0.014882 | 0.171141 | 0.032684 | -0.00786 |
| 0.088931 | 0.012013 | 0.154104 | 0.021123 | 0.000329 | 0.126225 | 0.012013 | 0.135371 | 0.031954 | -0.01078 | 0.16065 | 0.012013 | 0.144166 | 0.046064 | -0.0073 |
| 0.088931 | 0.009144 | 0.096025 | 0.038654 | -0.00163 | 0.126225 | 0.009144 | 0.106143 | 0.103855 | -0.0084 | 0.16065 | 0.009144 | 0.127791 | 0.245856 | -0.00788 |
| 0.088931 | 0.006275 | 0.07245 | 0.034139 | -0.00272 | 0.126225 | 0.006275 | 0.099104 | 0.049871 | -0.00656 | 0.16065 | 0.006275 | 0.125237 | 0.112557 | -0.00864 |
| 0.088931 | 0.003407 | 0.045055 | 0.025597 | -0.00261 | 0.126225 | 0.003407 | 0.083349 | 0.013837 | -0.00556 | 0.16065 | 0.003407 | 0.119479 | 0.009652 | -0.00811 |

Raw Data of 3 x-locations for 40Hz With Trip.